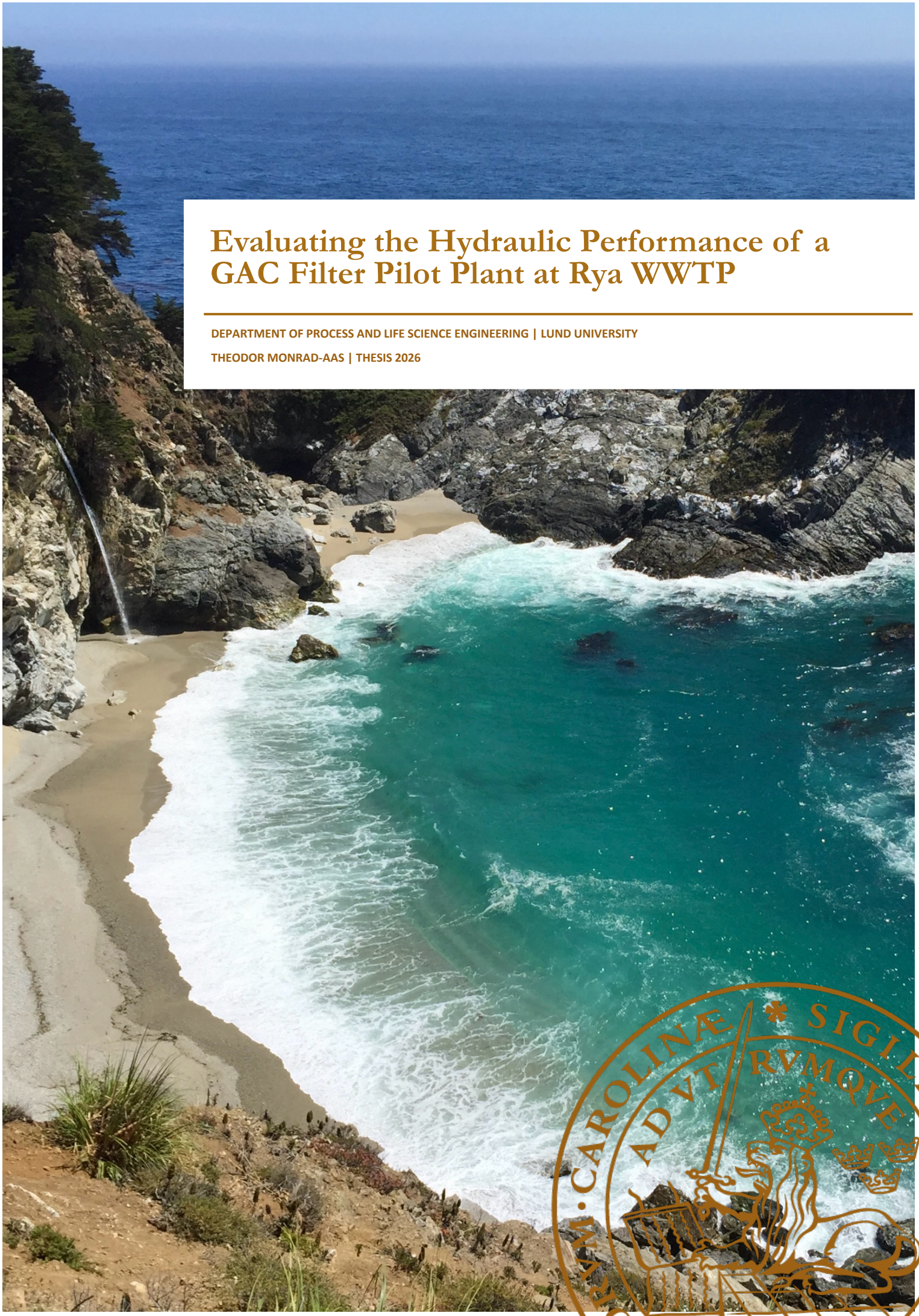

Evaluating the Hydraulic Performance of a GAC Filter Pilot Plant at Rya WWTP

DEPARTMENT OF PROCESS AND LIFE SCIENCE ENGINEERING | LUND UNIVERSITY

THEODOR MONRAD-AAS | THESIS 2026

Evaluating the Hydraulic Performance of a GAC Filter Pilot Plant at Rya WWTP

by

Theodor Monrad-Aas

Master Thesis number: 2026-12

Water and Environmental Engineering
Division of Chemical Engineering
Lund University

June 2026

Supervisor: **Associate professor Michael Cimbritz**
Co-supervisor: **PhD Alexander Betsholtz**
Examiner: **Associate professor Per Falås**

Picture on front page: McWay Falls, Big Sur, CA, USA, 2015 | Photo by: Theodor Monrad-Aas

Postal address
Box 124
SE-221 00 Lund, Sweden
Web address
http://www.ple.lth.se

Visiting address
Kemicentrum
Naturvetarvägen 14
223 62 Lund, Sweden

Telephone
+46 46-222 82 85
+46 46-222 00 00

Postal address
Box 124
SE-221 00 Lund, Sweden
Web address
http://www.ple.lth.se

Visiting address
Kemicentrum
Naturvetarvägen 14
223 62 Lund, Sweden

Telephone
+46 46-222 82 85
+46 46-222 00 00

Preface

This thesis marks the culmination of my studies in Chemical Engineering at Lund University's Faculty of Engineering (LTH).

I am sincerely grateful to my supervisor, Michael Cimbritz for inspiring me to pursue my master's thesis in the wastewater industry and connecting me with the remarkable team at Rya WWTP. I also extend my heartfelt gratitude to Alexander Betsholtz at Gryaab for his warm welcome. It has been a privilege to work together during my time with the GAC pilot project. The guidance, wisdom, and camaraderie I experienced during this time made my first experience in the field as an engineer a truly enjoyable and rewarding experience.

In addition, a special thank you to Amir Saeid Mohammadi and Britt-Marie Wilén at Chalmers University of Technology for generously providing the opportunity to access their laboratory facilities and equipment, which was instrumental in the completion of my experimental work.

Finally, I am deeply grateful to my family and friends for their unwavering encouragement from start to finish.

Populärvetenskaplig sammanfattning

Hög vattenåtgång sätter käppar i hjulet för nytt reningssteg mot mikroföroreningar på Ryaverket.

För att inte bryta mot ny EU-lag måste Ryaverket i Göteborg införa ett nytt reningssteg senast 2045. Målet är att bli av med flertalet ämnen som utgör risker för folkhälsan och miljön. Därför testar man nu ett så kallat kolfilter. Reningensprestandan fungerar hittills bra, men vad gör man om man tvingas använda upp stora delar av det renade vattnet för att rena själva kolfiltret?

Huvudsyftet med avloppsvattenrening är att skydda både folkhälsan och miljön. Genom att rena bort organiskt material, näringsämnen och smittämnen motverkas syrebrist, övergödning, och spridning av sjukdomar. Detta sker till stor del genom att naturens egna processer överförs till en kontrollerad och effektiv anläggning - ett avloppsreningsverk. Många ämnen, som industriella kemikalier, läkemedelsrester och PFAS släpps fortfarande ut orenade. Dessa brukar kallas mikroförereningar och kan också utgöra risker för folkhälsan och miljön. För att åtgärda detta har EU infört krav på att flertalet reningsverk ska rena ett urval mikroföroreningar senast 2045. Ryaverket, som renar avloppsvatten åt hundratusentals människor i Göteborg, måste hitta ett lämpligt alternativ för att inte bryta mot lagen. Därför har man byggt en testanläggning som utgörs av ett kolfilter bestående av en bädd med porösa kolpartiklar stora som grovmalet kaffe. Dessa kolpartiklar innehåller små porer som ger en stor yta där mikroföroreningarna kan fastna och separeras från vattnet.

Kolfiltret drivs på ett liknande sätt som en kaffebryggare - alltså genom att låta vatten pumpas upp och sippra igenom en bädd av partiklar med hjälp av gravitation under en viss tid. Till skillnad från vattnet i kranen, innehåller även det inkommande vattnet till kolfiltret partiklar som sätter igen bädden. Då ökar motståndet gradvis för vattnet att ta sig igenom bädden. Till slut måste vatten spolas åt andra hållet för att avlägsna partiklarna och luft kan också användas för att få bättre omblandning. Detta kallas backspolning och är något man inte vill göra för ofta då det förbrukar vatten som redan renats. Dessvärre har testanläggningen tvingats backspola upp till flera gånger per dag, vilket gör kolfiltret till ett mycket ineffektivt sätt att rena vattnet.

Inom detta examensarbete togs det fram en metod som kunde lokalisera motståndet för vattnet till toppen av bädden och därför avlägsnades det översta lagret. För att motverka återkomsten av motståndet och hålla prestandan i schack ökades intensiteten av backspolningen. Tyvärr återkom det stora motståndet. Den troliga orsaken är att mikroorganismer ställer till problem på grund av deras kolonialisation av kolfiltret. Denna tillväxt kan nämligen göra så att partiklar från det inkommande vattnet fastnar primärt högst upp där även de minsta kolpartiklarna återfinns. Sammantaget blockerar detta snabbt möjligheten för vattnet att ta sig förbi, vilket orsakar en kort reningstid och tvingar kolfiltret till att backspola ofta. Detta får en förödande effekt på effektiviteten hos ett kolfilter och är något avloppsreningsverk bör undersöka så att de inte måste rena anläggningen mer än vattnet.

Summary

The implementation of the revised urban wastewater treatment directive (UWWTD) introduced mandatory micropollutant abatement or quaternary treatment for many wastewater treatment plants (WWTPs) within the EU. Rya WWTP in Gothenburg, which is treating almost 880,000 PE of water, must find and implement a suitable option by 2045 at the latest. One alternative is granular activated carbon (GAC) which was previously pilot tested, but the results were inconclusive. Therefore, a new GAC pilot plant was commissioned and has been running since July of 2025. It has an EBCT of 22 min, a bed height of 2.7 m, filter area of 1 m^2 and influent flow rate of 7.5 m^3/h. The GAK pilot plant has exhibited deteriorating hydraulic performance over an extended period, with filter run times decreasing from an average of ca 12 hours to 3 hours with low TSS loads before backwashing. Therefore, this thesis was primarily aimed at evaluating, localising and combatting the poor hydraulic performance, and secondarily to evaluate the treatment performance in relation to the revised UWWTD, standard parameters and PFAS-24.

A method was developed that successfully localised and quantified the pressure drop for GAC from different depths of the bed. By tracking changes in hydraulic resistance over time, it could be concluded that the main hydraulic bottleneck was localised to the top of the GAC bed. Following remediation of the problem, the filter run time improved to a mean of 24 h. However, despite more aggressive backwashing and mass balances that indicated TSS were overall removed from the GAC filter, the deterioration in the hydraulic performance resurged after three weeks. Particle size distribution (PSD) analysis confirmed stratification of the bed which can contribute to surface filtration and rapidly increasing pressure drop. Because mean influent TSS concentration and filter run time only showed weak to no correlation, along with a presence of biofilm in the GAC filter and on the particles, significant DO and BOD removal as well as indications of nitrification suggests the problem is associated with biofilm growth. The MP abatement performance was still in accordance with the UWWTD after ~12,000 treated bed volumes (BV) with 86% elimination based on the best combination of substances. However, treatment performance for PFAS-24 reached below 80% already at ~5,000 treated BV.

Sammanfattning

Införandet av det reviderade avloppsdirektivet (UWWTD), introducerade krav på rening av mikroföroreningar eller kvartär rening för många avloppsreningsverk i EU. Ryaverket i Göteborg, som renar vatten motsvarande nästan 880 000 personekvivalenter måste därmed hitta och införa en lämplig lösning senast 2045. Ett alternativ är granulärt taktivt kol (GAK), som tidigare testats i en pilotanläggning, men resultaten var inte entydiga. Därför startades ett nytt GAK-pilotprojekt som har pågått sedan juli 2025. Den har en EBCT på 22 minuter, en bäddhöjd på 2,7 m, en filterarea på 1 m² samt ett inflöde på 7,5 m³/h. GAK-pilotanläggningen har under en längre period uppvisat en försämrad hydraulisk prestanda med filterdriftstider som har sjunkit från ett medelvärde på cirka 12 timmar till 3 timmar med låga TSS-belastningar innan backspolning. Därför syftade denna avhandling i första hand till att utvärdera, lokalisera och åtgärda den dåliga hydrauliska prestandan, och i andra hand till att utvärdera reningsprestandan i förhållande till den reviderade UWWTD, standardparametrar och PFAS-24.

En metod utvecklades som framgångsrikt lokaliserade och kvantifierade tryckfallet för GAK från olika djup. Genom att följa förändringar i det hydrauliska motståndet över tid kunde man dra slutsatsen att den huvudsakliga hydrauliska flaskhalsen var lokaliserad till toppen av GAK-bädden. Efter åtgärdande av problemet förbättrades filterdriftstiden till ett medelvärde på 24 timmar. Trots mer aggressiv backspolning och massbalanser som indikerade att TSS överlag avlägsnades från GAK-filtret, återkom försämringen av den hydrauliska prestandan efter tre veckor. Analys av partikelstorleksfördelningen (PSD) bekräftade en stratifiering av bädden, vilket kan bidra till ytfiltrering och ett snabbt ökande tryckfall. Eftersom den genomsnittliga TSS-koncentrationen i inflödet och filterdriftstiden endast visade svag till ingen korrelation, tillsammans med förekomsten av biofilm i GAC-filtret och på partiklarna, tyder en betydande minskning av DO och BOD samt tecken på nitrifikation på att problemet är förknippat med biofilmstillväxt. Reningsprestandan för direktivämnena var fortfarande i enlighet med det reviderade avsloppsdorektivet efter ~12 000 behandlade bäddvolymer (BV) med 86 % eliminering baserat på den bästa kombinationen av substanser. Reningsprestandan för PFAS-24 nådde under 80 % redan vid ~5 000 behandlade BV.

Table of Contents

List of Abbreviations

AS	Activated sludge
BOD	Biochemical oxygen demand
BV	Bed volumes
COD	Chemical oxygen demand
EBCT	Empty bed contact time
DO	Dissolved oxygen
GAC	Granular activated carbon
MBBR	Moving bed bioreactor
MP	Micropollutant
MTZ	Mass transfer zone
NH_4-N	Ammonium nitrogen
NO_2-N	Nitrite nitrogen
NO_3-N	Nitrate nitrogen
N_{tot}	Total nitrogen
PE	Population equivalent
PFD	Process flow diagram
PSD	Particle size distribution
PO_4-P	Phosphate phosphorus
P_{tot}	Total phosphorus
PFAS	Per- and polyfluoroalkyl substances
TOC	Total organic carbon
TSS	Total suspended solids
UVA_{254}	Ultraviolet Absorbance at 254 nm
UWWTD	Urban wastewater treatment directive
WWTP	Wastewater treatment plant

1 Introduction

Virtually any chemical utilised in modern society has the potential to eventually enter the wastewater stream as urban wastewater can be a combination of domestic, industrial as well as stormwater runoff in combined sewer systems (Lofrano and Brown, 2010). In this complex water matrix, certain pollutants are unsuccessfully removed by conventional treatment steps at wastewater treatment plants (WWTPs) as they are not designed for this purpose (Schölzel et al., 2022). Therefore, an additional treatment step, specifically targeting residual micropollutants (MPs) addresses this issue (Pistocchi et al., 2022).

In 2025, the revised Urban Wastewater Directive (UWWTD), Directive (EU) 2024/3019 introduced mandatory MP abatement for many WWTPs in all member states with 12 key substances serving as indicators, with an aim of 80% removal. This stage, referred to as quaternary treatment, must be implemented at relevant WWTPs by 2045 at the latest (European Parliament and Council of the European Union, 2024). Several options exist for WWTPs to implement quaternary treatment. The most mature technologies are ozonation and those based on adsorption, e.g. powdered activated carbon (PAC) and granular activated carbon (GAC) or a combination of two processes (Pistocchi et al., 2022). All have been shown to successfully reach 80% elimination of the key indicators at full-scale WWTPs in Switzerland (Wunderlin & Bitterwolf, 2025). Outside the 12 indicator substances in the UWWTD, treatment requirements may also be triggered for additional MPs, such as PFAS, if local assessments determine their discharge presents a risk to the environment or human health (European Parliament and Council of the European Union, 2024).

Among WWTPs in Sweden, Rya WWTP in Gothenburg is treating around 880,000 PE and will be affected by the legislation. The WWTP must find a suitable option to implement quaternary treatment, but is limited by its physical footprint. Both ozonation and GAC are the options currently being considered at Rya WWTP as the quaternary treatment step and they each have advantages and disadvantages. Ozonation could be beneficial as it is less expensive to build from scratch compared to GAC (Rizzo et al., 2019). However, ozonation can produce oxidation by-products and transformation products which could be problematic from a toxicological perspective and could therefore require subsequent polishing, which increases the footprint and costs (Bourgin et al., 2018; Pistocchi et al., 2022; Ianes et al., 2025). For GAC, after higher initial construction costs, the major cost driver is the frequency of GAC reactivation (Rizzo et al., 2019; Pistocchi et al., 2022; Ianes et al., 2025). This must be investigated as the time until breakthrough can vary considerably (Benstoem et al., 2017). In addition, GAC has been seen to remove some PFAS in water treatment applications (Appleman et al., 2014; McCleaf et al., 2017). In contrast, ozonation has demonstrated poor efficiency for PFAS removal, which is problematic should it become a future treatment requirement (Xin et al., 2024).

To find the best quaternary treatment alternative, a GAC filter pilot, hereinafter referred to as a ‘GAC pilot’, was tested at Rya WWTP between 2022-2024, but due to issues with its design, representable conclusions could not be drawn. Thus, a new GAC pilot was developed and taken into operation in July of 2025 and is set to run until at least the end of 2026. The aims with the GAC pilot are to investigate how it performs as the final treatment step in the process and how long the GAC filter can successfully maintain sufficient treatment to be in accordance with the

UWWTD before reactivation is required. Additional key factors to investigate are the water usage for backwashing and the performance in relation to PFAS removal to evaluate if it can be used for potential future PFAS treatment requirements. However, the GAC pilot has been experiencing issues regarding its hydraulic performance, with very short filter run times resulting in frequent backwashing. Current research on GAC filters primarily focuses on MP removal and the longevity of adequate treatment performance. However, for successful large-scale implementation, the hydraulic performance can be highly detrimental to economical operation (Schölzel et al., 2022). Therefore, it is equally important to evaluate GAC filters from a hydraulic perspective, which will be the primary focus of this thesis.

1.1 Aim

The overarching aim of this thesis is to evaluate and test strategies to improve the hydraulic performance of the GAC pilot at Rya WWTP. The secondary aim is to evaluate the removal of MPs and relevant wastewater nutrients to date. Within the scope of this master thesis, the exact timeframe before reactivation of GAC is needed cannot be established.

What will be evaluated more specifically are:

- How influent TSS concentration affects the filter run time.
- How the hydraulic performance changes over time.
- Whether more aggressive backwashing programs can improve hydraulic performance.
- What a suitable frequency, duration and strategy for backwashing is.
- How treatment varies with the number of bed volumes treated and whether there are any differences between substances in terms of removal.
- To what extent standard parameters e.g. TSS, DOC, N-tot, and P-tot are removed.

The thesis will be primarily based on experiences during the period from February to May 2026 when the author became involved with the pilot testing. It will also consider the preceding period from June 2025 to January 2026.

2 Revised UWWTD Compliance at Rya WWTP: GAC Adsorption Theory & Design

The revised Urban Wastewater Directive (UWWTD) will be presented and what it entails in relation to implementing quaternary treatment at Rya WWTP. Next, an overview of the current treatment process at Rya WWTP will be given to provide some context on where the proposed GAC filter would fit in and to gain greater understanding on the upstream process steps that may affect it. Then follows a theoretical explanation on how GAC filters operate and some key GAC filter design guidelines will be presented.

2.1 The Revised UWWTD

As one of the frontrunners in micropollutant abatement, Switzerland enacted legislation to combat certain substances on January 1, 2016. The aim is 80% removal of a selection of 12 substances (10 pharmaceuticals and 2 industrial chemicals) that serve as key indicator compounds because they are ubiquitous parent compounds (not degradation products) that are continuously discharged into wastewater and measurable with standard analytical methods. In addition, they are difficult to remove biologically at WWTPs (<50% removal) and can be removed by either activated carbon or ozonation (Wunderlin & Bitterwolf, 2025). These substances can be seen in Table 2.1 divided across two categories.

Table 2.1. The 12 substances from the UWWTD divided across the two categories.

	Indicator Substance	**Application**
Category 1	Amisulpride (CAS-nr 71675-85-9)	Antipsychotic drug
	Carbamazepine (CAS-nr 298-46-4)	Anticonvulsant drug
	Citalopram (CAS-nr 59729-33-8)	Antidepressant
	Clarithromycin (CAS-nr 81103-11-9)	Antibiotic
	Diclofenac (CAS-nr 15307-86-5)	Anti-inflammatory drug
	Hydrochlorothiazide (CAS-nr 58-93-5)	Diuretic drug
	Metoprolol (CAS-nr 37350-58-6)	Cardiovascular drug
	Venlafaxine (CAS-nr 93413-69-5)	Antidepressant
Category 2	Benzotriazole (CAS-nr 95-14-7)	Anti-corrosion agent
	Candesartan (CAS-nr 139481-59-7)	Antihypertensive drug
	Irbesartan (CAS-nr 138402-11-6)	Antihypertensive drug
	Mixture of 4-methylbenzotriazole (CAS-nr 29878-31-7) and 5-methylbenzotriazole (CAS-nr 136-85-6)	Anti-corrosion agent

Exactly nine years later, a revised Urban Wastewater Directive (UWWTD) came into effect within the European Union on January 1, 2025. The overarching aim of the UWWTD, Directive (EU) 2024/3019, is to strengthen the protection of the environment and public health, reduce greenhouse gas emissions and promote a circular economy in line with EU's action plan on zero pollution of air, water and soil. In part, the directive entails more stringent tertiary treatment,

meaning lower nitrogen and phosphorous levels at more WWTPs. For the first time, it also introduces mandatory quaternary treatment (Article 8) to combat certain micropollutants. The same 12 indicator substances as in the Swiss legislation are used, see Table 2.1.

To be in accordance with the UWWTD, at least six indicator substances should be selected, out of which the number of Category 1 substances should be twice that of the Category 2 substances. For the selected MPs, treatment should remove at minimum 80% (annual average) calculated based on the dry weather influent flow across the entire WWTP process. To finance this, producer responsibility was also introduced. It stipulates that producers of drugs and cosmetics should bear at minimum 80% of the costs associated with removing MPs at WWTPs (European Parliament and Council of the European Union, 2024; Naturvårdsverket, 2026).

According to the UWWTD, quaternary treatment should be enforced at WWTPs with a load at or above 150,000 person equivalents (PE) and those from 10,000 PE following risk assessment. It must be implemented at all relevant WWTPs by the year 2045 in EU member states. However, this transition is gradual for WWTPs from 150,000 PE, where 20% should be in accordance with the directive already by 2033 and 60% by 2039 (European Parliament and Council of the European Union, 2024; Naturvårdsverket, 2026).

In addition, Article 8 stipulates that national risk areas be designated by the end of 2030 where the concentration and accumulation of micropollutants from WWTPs present a risk to the environment or to human health. This could trigger treatment requirements for substances outside the 12 indicator substances in the revised UWWTD. For instance, PFAS, which are designated as priority substances and assigned an environmental quality standard under Directive 2013/39/EU, could also require quaternary treatment. (European Parliament and Council of the European Union, 2013; European Parliament and Council of the European Union, 2024).

The Revised UWWTD and Rya WWTP

On a national level in Sweden, there are several WWTPs affected by the UWWTD, among them are Rya WWTP in Gothenburg. Rya WWTP is currently treating almost 880,000 PE of wastewater and does not yet employ quaternary treatment (Videbris, 2025). The Swedish Environmental Protection Agency (Swedish EPA) were given the assignment to propose necessary revisions for the implementation of the UWWTD and to aid in its implementation. They have, recently at the time of writing, submitted a document with proposals for legislative amendments necessary to implement it and an impact assessment of the proposed legislative amendments. Based on this document it remains unclear if Rya WWTP will be included in the first 20% of WWTPs required to implement quaternary treatment by 2033 (Naturvårdsverket, 2026). Regardless, it is necessary to explore options for suitable quaternary treatment alternatives for future compliance.

2.2 The Treatment Process at Rya WWTP

The current process at Rya WWTP is quite unconventional due to space limitations and progressive upgrading of the plant to be meet more stringent treatment requirements. Therefore, a short overview of the treatment process employed at Rya WWTP (Videbris, 2025), see Figure 2.1, will be presented.

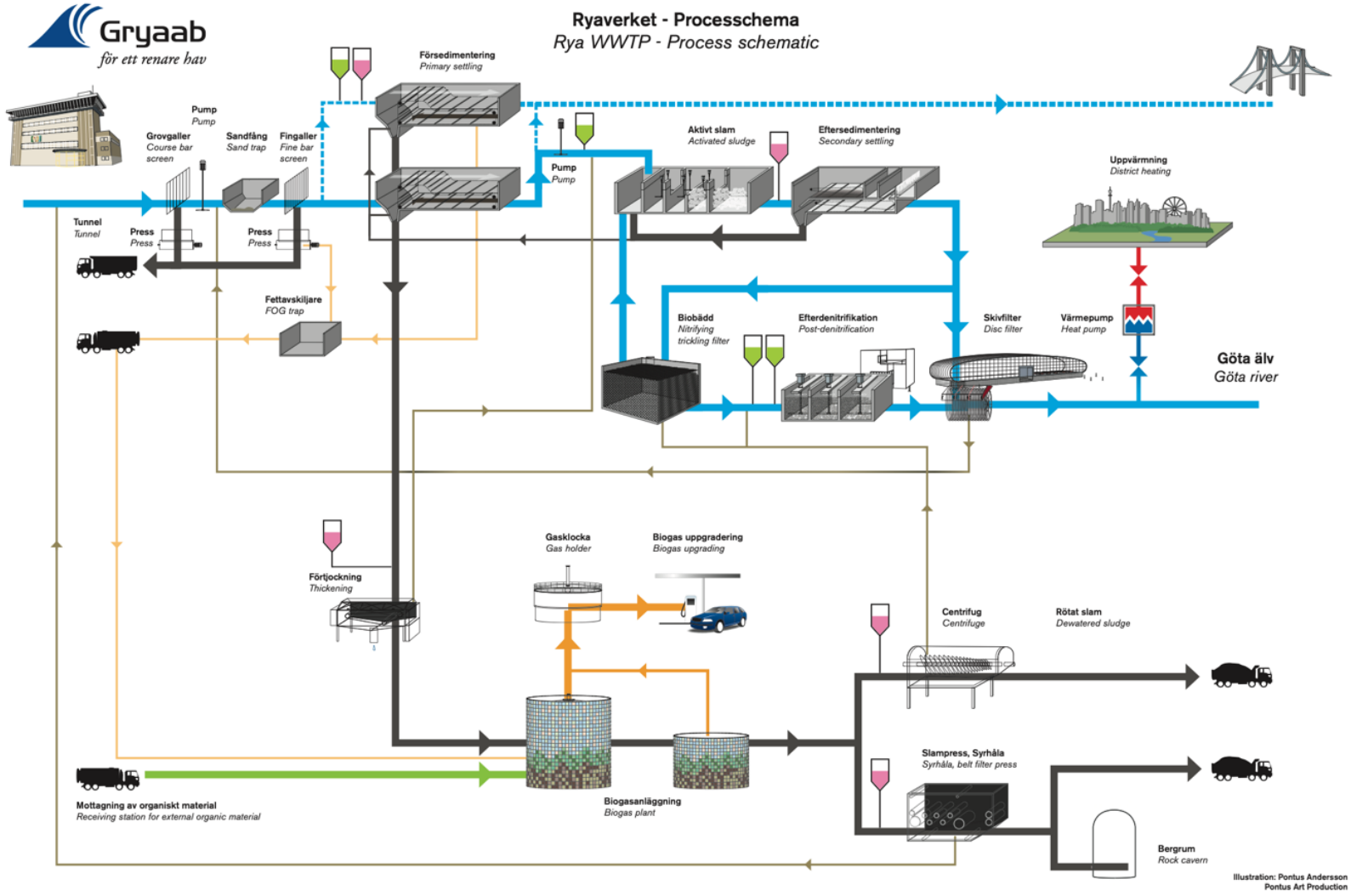

Figure 2.1. Overview of the current treatment process at Rya WWTP (Gryaab 2026, with permission).

The first step consists of mechanical treatment where aerated sand traps separate heavy inorganic particles followed by fine screens. The water is then lead to several sedimentation basins for primary treatment where solid particles are separated as primary sludge. Following primary treatment, there are different forms of biological treatment. There are both activated sludge (AS) treatment and attached-growth treatment (nitrifying trickling filters) and carrier-based treatment for post-nitrification and post-denitrification. The effluent from primary treatment is mixed with recycled AS and recirculated water from the nitrifying trickling filters, which then enters activated sludge treatment as the first step of biological treatment. Rya WWTP employs simultaneous precipitation with iron sulphate to remove phosphorus as iron phosphate, which is subsequently removed with the sludge in the secondary clarifiers. To enhance the flocculation properties, polymers are also added.

The AS treatment itself is highly loaded and aims at denitrification and BOD removal. The sludge settling characteristics governs the hydraulic capacity and normally permits about 8-9 m^3/s, but up to 10 m^3/s under favourable conditions is possible. If the capacity of the AS treatment step is exceeded, the excess flow can be entirely bypassed or direct precipitation with poly aluminium chloride and polymers be utilised. The effluent from AS treatment enters the secondary clarifier basins and most of the sedimented sludge is recycled to the AS treatment basins, whereas the excess sludge is led to the primary treatment basins. The effluent from the secondary clarifiers has different fates depending on the influent flow. During normal flows, the majority is routed to the nitrifying trickling filters and then recycled back to either AS treatment or to post-denitrification. However, during high flows increasingly more water is directed to post-nitrification to prevent overloading the secondary clarifiers and increase throughput. The remaining water from the clarifiers is routed directly to the disc filters.

As can be imparted from above, nitrification is carried out by nitrifying trickling filters and/or post-nitrification with carriers. The nitrifying trickling filters are filled with corrugated immobile plastic material and can treat up to 7 m^3/s water. The post-nitrification basins instead employ moving plastic carriers in the form of moving bed biofilm reactors (MBBR) that have a capacity of 5 m^3/s.

Apart from the denitrification in the AS treatment process, post-denitrification basins in the form of MBBRs are also used to primarily treat the effluent from the post-nitrification step. Here, methanol is used as the external carbon source. The post-denitrification has a total hydraulic capacity of 4 m^3/s.

The final step prior to effluent discharge to Rya Nabbe are disc filters at 15 μm which are used to remove residual suspended solids. Based on design suspended solids loads, the 32 filters have a capacity of 8 m^2/s. During high flows they can be bypassed. Cleaning in place is done using sodium hypochlorite or hydrochloric acid.

2.3 GAC Adsorption Theory & Design

GAC filters are based on adsorption and have been used for almost a century in drinking water treatment, primarily for odour, colour and taste remediation. Because their large internal surface area allows them to adsorb micropollutants, GAC filters have recently become a key technology for MP abatement in wastewater treatment. The idea is to use a bed consisting of activated

carbon granules and allow water to flow through the filter at a sufficient residence time. There are several possibilities for the mode of operation of a GAC filter. They can be gravity driven (downflow) or pressurised. The bed itself can be fluidised, with only absorption and minimal solids retention or fixed, leading to both adsorption and solids retention. GAC filters can be operated continuously or discontinuously (with or without intermittent backwashing). Although drinking water treatment has used GAC filters for decades, the design principles are not directly transferrable to WWT and thus require further consideration for implementation (Çeçen & Aktaş, 2011, Schölzer et al., 2022).

2.3.1 Adsorption with GAC in Wastewater Treatment

A brief overview of the production process, structure and adsorption with GAC will be presented.

Production Process and Structure of GAC

In wastewater treatment, activated carbon is the most common type of solid adsorbent and the adsorbates are typically dissolved organic substances and certain inorganic substances present in the water. Activated carbon is a highly porous carbonaceous material with a vast internal surface area (500-1,500 m^2/g) available for adsorption (Çeçen & Aktaş, 2011). It can be produced from a variety of carbon-rich raw materials, e.g. coal, coconut shells or wood. The production process first involves carbonisation, where the volatile components escape as gas, leaving a carbon-rich structure. The ensuing step is thermal or chemical activation, resulting in pores that comprise a network of different sizes. The choice of starting material along with the activating agent and conditions during the production process has a profound impact on the characteristics and performance of the activated carbon manufactured (Goyal & Chand, 2005; Çeçen & Aktaş, 2011). Structurally, activated carbon consists of aromatic sheets of hexagonal carbon rings similar to graphite, but with less order and greater interlayer spacing (Goyal and Chand, 2005). Together they form microcrystalline structures that are interconnected via functional groups (Çeçen & Aktaş, 2011). The irregular arrangement and physical gaps between the aromatic sheets result in a porous structure. Adsorption occurs in all pore sizes. The macropores (> 50 nm) and mesopores (2-50 nm) serve mainly as diffusion transport networks to the micropores (< 2 nm), which constitute ~95% of the surface area for adsorption (Goyal and Chand, 2005). The activated carbon is typically turned into granules between 0.2-5 mm in diameter by crushing or made from pulverised activated carbon using binders (Çeçen & Aktaş, 2011).

Adsorption with GAC

The hydrophobic effect partitions substances toward the activated carbon, which together with attractive van der Waals interactions (physisorption) and chemical interactions (chemisorption) result in separation by adsorption (Çeçen & Aktaş, 2011). Isotherms describe the equilibrium relationship between the adsorbate remaining in the liquid phase and the amount adsorbed onto the solid phase at a constant temperature (Tchobanoglous et al., 2003). However, different substances can have varying affinity for the GAC depending on their size, weight, solubility, polarity, charge, structure and functional groups, leading to competition for the adsorption sites (Çeçen & Aktaş, 2011). Adsorption with GAC is typically rate-limited by external and intraparticle mass transfer, which are dependent on the flow rate, particle size and pore structure of the GAC (Çeçen & Aktaş, 2011). As increasingly more water is treated, the primary zone for adsorption, i.e. the mass transfer zone (MTZ) for each specific substance will gradually

move further into the bed at varying rates as the GAC filter becomes saturated. Eventually, the MTZ for some adsorbates reaches the bottom of the filter which leads to breakthrough (Tchobanoglous et al., 2003; Benstoem et al., 2017). The GAC bed must then be replaced once breakthrough becomes unacceptable (hits minimum treatment target). The spent GAC can be regenerated (removal of adsorbates) or reactivated (destruction of adsorbates and new activation) (Çeçen & Aktaş, 2011).

2.3.2 Solids Retention and Backwashing GAC Filters

Different modes of filtration and the principles behind backwashing will be presented.

Solids Retention Mechanism and Pressure Drop

To drive filtration, a driving force in the form of a pressure difference is required, which can be achieved by e.g. pumps or gravity (Schölzel et al., 2022). The focus here will be solely on gravity driven (downflow) GAC filtration.

The porous bed created by the GAC particles in a fixed-bed GAC filter will retain solids. In addition to the inherent hydraulic resistance from the filter medium itself, the retention of solids on or in the filter medium during filtration decreases the available driving force, which results in an increase in the pressure drop across the filter (Δp). However, the rate at which pressure drop develops with the volume filtered (V) varies based on the mode of filtration (Ripperger et al., 2012). In general terms, for cake filtration, where the cake itself is the filter, the pressure drop develops linearly as the cake grows. If the interparticle voids of the filter medium are smaller than the particles in the influent, as in surface filtration, they are increasingly blocked at the surface because the interparticle voids are smaller than the solids. This typically leads to a rapid non-linear pressure drop development. In depth filtration, particle retention is achieved by different mechanisms depending on their size. Particles in the influent larger than (above 10 μm) the interparticle voids are trapped mechanically, causing a pressure drop behaviour similar to surface filtration. Particles between 1-10 μm are transported via inertia effects and adhere to the surface of the filter grains due to sterical stabilisation and surface forces. For particles below 0.1 μm Brownian diffusion is the primary transport mechanism to the grain surface followed by adhesion because of surface forces. For particles between 0.1-1 μm the transport by inertia and Brownian diffusion is small, thus this size interval exhibits the least retention in depth filters. As more particles adhere to the filter grains, the local interparticle void size decreases, which increases the pressure drop of the filter media with filtrate volume (Ripperger et al., 2012).

Backwashing of Discontinuous GAC Filters

During filtration, solids in the influent are retained by the filter which gradually increases the hydraulic resistance of the bed. Therefore, a complete filter cycle for discontinuous filters is characterised by the filter run (active filtration) until a certain threshold is reached. This triggers a cleaning phase, i.e. backwashing program in between filter runs, to restore the hydraulic and solids holding capacity. Backwashing consists of a combination of phases that use washing with treated water and/or scouring with air in the opposite direction (Schölzel et al., 2022). Flushing water upwards results in a drag force that overcomes the gravitational force, which increases the interparticle pore space and results in overall expansion of the bed. Bed expansion typically increases with higher water velocities and lower temperatures. The resulting shear forces breakoff solids which are then removed with the water. For well-functioning backwashing

programs, pumping water upwards will eventually lead to stratification of the bed. This means small particles will fluidise more than larger particles at the same flow rate during backwashing. Once the backwashing stops, the larger particles will sink faster than the smaller particles, altogether leading to sorting by settling velocities (Crittenden et al., 2012; Schölzel et al., 2022).

In addition to backwashing with water, air scouring is typically also used to enhance agitation and break up filter clogging from adhesive wastewater solids. (Cleasby, 1974). However, air scouring can lead to abrasion of the GAC particles and sufficient hardness of the chosen GAC therefore becomes important (Schölzel et al., 2022). Other benefits of backwashing programs are removal of gas and air pockets, smoothing of the filter surface and elimination of fine grains from commissioning or filter material abrasion. There are different criteria or combinations of criteria that can be used to signify the end of the filter run and trigger the backwash program. For instance, reaching a set filtration time interval, a certain flow rate, desired terminal pressure drop or concentration condition. (Schölzel et al., 2022). It is important to consider the increase in the hydraulic load in a WWTP if backwashing water is directly recycled upstream at the flow rate used during backwashing. The alternative is a storage tank with adequate capacity that allows gradual return of spent backwashing water (Cleasby & Baumann, 1974).

2.3.3 GAC Filter Design – A Balance Act of Competing Interests

Important considerations for design and factors that could influence the operation of a GAC filter at Rya WWTP will be presented.

Empty Bed Contact Time (EBCT)

The primary design parameter for GAC filters is the Empty Bed Contact Time (EBCT), i.e. the residence time of water in the bed without accounting for the volume occupied by GAC. This means the effective contact time during operation is shorter and dependent on the bed porosity (Fundneider et al., 2021a). The EBCT is defined as:

$$\text{EBCT} = \frac{h_{bed}}{v_{filter}} = \frac{A_{bed} \times h_{bed}}{A_{bed} \times v_{filter}} = \frac{V_{bed}}{Q}$$

where A_{bed} is the cross-sectional area of the filter bed and h_{bed} the height of the filter bed, V_{bed} is the empty volume of the filter that is to be filled with GAC, v_{filter} is the filter velocity and Q the influent flow rate.

The EBCT is often recommended to be between 20-30 minutes to allow sufficient contact time (Fundneider et al., 2021a) at maximum flow and with n-1 filters in operation. It is advised to have at least 4 filter cells to ensure redundancy during maintenance or reactivation. From the equation, the EBCT is governed by the relationship between the height of the bed and the filter velocity. It is recommended that the bed is between 1.5 – 3.0 m and the filter velocity below 9 m/h (Böhler et al., 2023). To maintain the desired EBCT, the flow must be constant (constant-rate filtration). Thus, to account for the increase in pressure drop, this can be accomplished by increasing the height of the water column (overflow control) or by incrementally opening a valve (outlet control) (Cleasby and Baumann, 1974; Schölzel et al., 2022).

Treated Bed Volumes

The total volume of treated water ($V_{treated}$) is often normalised by the bed volume (V_{bed}) and used as a proxy for operating time. The treated bed volumes (BV) can be calculated according to:

$$BV = \frac{V_{treated}}{V_{bed}}$$

The achievable service life as treated BV to maintain sufficient treatment in accordance with the directive is not a set number, and is partly dependent on the water matrix, like the DOC concentration (Juarez et al., 2026). However, attainable values based on adequate removal of UWWTD substances are typically in the range of 20,000-30,000 BV from experience (Böhler et al., 2023). There are examples of GAC filters that sufficiently treat MPs even over 40,000-50,000 BV in Sweden (Busck et al., 2026).

Grain Size, Biofilm Growth and Pre-treatment

The chosen grain size interval of the particles is important to consider. Smaller particles incur less mass transfer limitations, which is positive from an adsorptive performance standpoint (Çeçen & Aktaş, 2011). However, it could have impacts on the hydraulic performance of the GAC filter. Conversely, larger particle sizes result in deeper beds being needed for a similar mass of GAC. Because the particles are more mass transport limited, the achievable lifespan before it needs to be replaced is typically lower, which results in higher operating costs than for smaller GAC size intervals (Böhler et al., 2023).

The nature of the influent to GAC filters will result in them acting as a combination of surface and depth filtration. The favourable pressure curve, i.e. the desired behaviour of the retention in the bed, is an initially proportional response for the pressure drop curve with increasing filtrate volume that then transitions to an approximately linear response (Schölzel et al., 2022). If the bed has been stratified, smaller particles are concentrated at the top, which translates to smaller flow channels. Therefore, the resistance to flow and most of the pressure drop is likely to occur at the top section of the bed. This also means the main point of retention of solids will also be in the top layer of the bed, which can result in surface filtration that causes a rapidly increasing pressure drop curve, shorter run times and less TSS being captured per run (Schölzel et al., 2022). To achieve better bed utilisation, surface filtration can be mitigated by selecting a GAC type with a larger and more uniform grain size, minimising fines, changing the flow direction or using higher filtration rates (at the detriment of higher initial pressure drop). Increasing the maximum available pressure drop will also increase filter run times and compensate for surface filtration. (Cleasby & Baumann, 1974; Crittenden et al., 2012; Schölzel et al., 2022). Figure 2.2 shows an example of how the pressure drop curve changes to a more pronounced surface filtration appearance at low filtration rates.

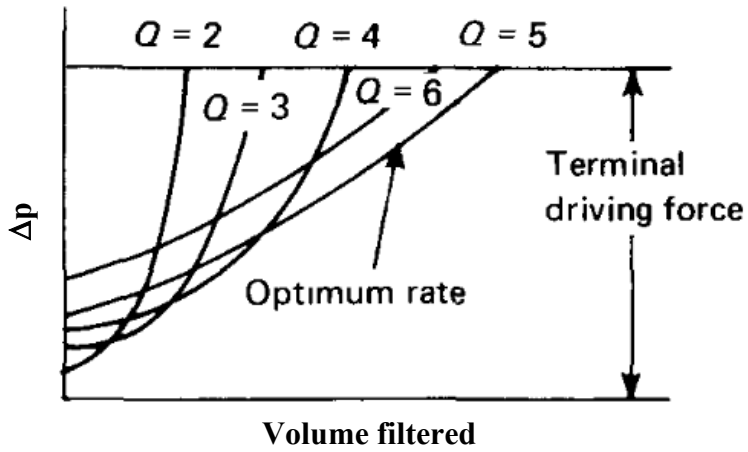

Figure 2.2. How the pressure drop development for combined surface filtration and depth filtration changes with volume filtered for different filtration rates (Q) for constant rate filtration systems. Adapted from (Cleasby & Baumann, 1974).

Biofilm growth can develop on the granules in a GAC filter, which can contribute to the removal and transformation of biodegradable organic substances and MPs (Çeçen & Aktaş, 2011; Betsholtz 2023; Takman et al., 2024). However, excessive biofilm can also lead to clogging of the filter which exacerbates the hydraulic performance of the GAC filter. This causes more frequent backwashing and can contribute to the surface filtration effect. Several factors can influence biomass growth including influent biomass concentration, nutrient availability, contact time, type of GAC, water temperature and the backwash protocol (Fundneider et al., 2021b; Schölzel et al., 2022).

An average influent particle content below 20 mg TSS/L has been recommended to prevent short filter runs, and it is preferable to achieve a minimum filter run time of at least 24 h for economical operation. (Schölzel et al., 2022). The achievable filter run time ranges from several hours to weeks or months. Generally, better pre-treatment is considered vital in obtaining longer filter run times (Schölzel et al., 2022; Svahn & Borg, 2024; Juarez et al., 2026). For example, implementing membrane filtration prior to a GAC filter can increase the run times substantially as the influent TSS concentration becomes negligible, but biofilm growth still occurs and the GAC filter will eventually require backwashing (Fundneider et al., 2021b).

3 Materials & Methods

The setup and design of the GAC pilot will first be presented followed by how the hydraulic and treatment performance were assessed.

3.1 The GAC Filter Pilot Setup and Design

The setup and design of the GAC pilot at Rya WWTP will be presented.

3.1.1 GAC Pilot Setup

The GAC pilot at Rya WWTP was developed by Eliquo Malmberg water and was taken into operation during the summer of 2025. It is a gravity driven downflow type filter with a total height of 4 m, an internal height of 3.75 m, with an overflow channel at 3.55 m, see Table 3.1 for dimensions. The cross-sectional geometry is square with an area of 1 m^2. The filter bottom consists of three Malmberg Triton® bottoms, with slit openings of 0.2 mm, which corresponds to half the diameter of the smallest GAC granule fraction (0.425 mm) of the chosen GAC-type. The bed itself is filled with GAC of type Cyclecarb® 401 from Chemviron, some important characteristics can be seen below in Table 3.2 (Chemviron, 2020a; Chemviron, 2020b). When it was commissioned the intentioned design EBCT was 20 min with a filter bed height of 2.5 m resulting in a 7.5 m^3/h flow. Almost 1.125 kg (1.118 kg) of Cyclecarb® 401 was added, which should correspond to 2.5 m^3 (2.5 m) of GAC. However, the resulting obtained bed height was around 2.7 m when the GAC was started. Thus, the resulting EBCT was slightly higher at about 21.6 min. With a bed height of 2.7 m, the distance to the overflow was 1.05 m.

Table 3.1. Summary of important GAC filter dimensions and design values

Total height (m)	4.00
Internal height to upper edge (m)	3.75
Height to overflow channel (m)	3.55
Filter area (m^2)	1
Bed height (m)	2.7
Flow rate (m^3/h)	7.5
Filter velocity (m/h)	7.5
EBCT (min)	21.6

Table 3.2. Summary of important Cyclecarb® 401 properties.

Bed Density (kg/m^3)	450
Grain size interval (mm)	0.425 - 2.36 (US Sieve Series 8 x 40)
	>2.36 (max 10 wt%)
	<0.425 (max 5 wt%)
Mean particle diameter (mm)	1.1
Pressure loss per meter bed (mbar/m)	~ 22 (at 7.5 m^3/h and 10°C)
	~ 18 (at 7.5 m^3/h and 25°C)

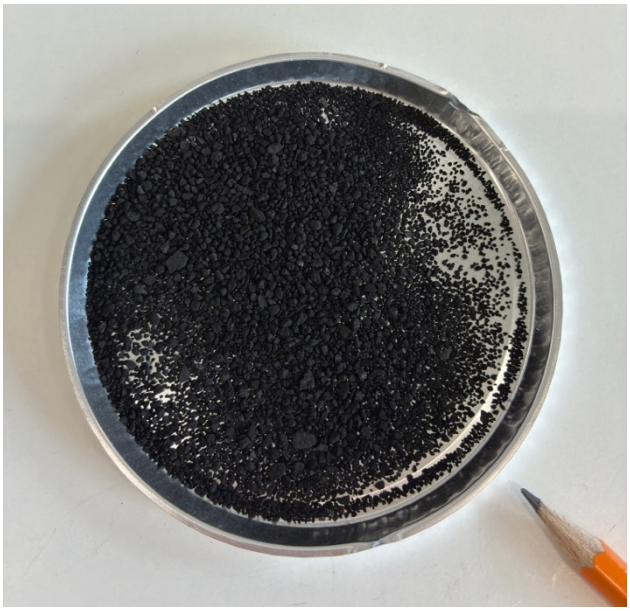

Figure 3.1. New GAC particles laid out on an aluminium dish with a pencil as size reference.

In Figure 3.2 a simplified process flow diagram can be seen of the process and Figure 3.3 shows the GAC pilot itself. The water is pumped from the flow channel following the disc filters into an IBC tank. The flow channel is equipped with a turbidity sensor for measuring TSS concentration. Constant flow must be maintained to achieve the desired EBCT. The set water level determines the max available head and by gradually opening the effluent control valve the effective head changes depending on the hydraulic resistance of the bed so that the flow rate is maintained. The treated water enters an effluent tank from which it can be routed back to flow channel or to a 15 m^3 tank holding backwashing water. Differential pressure can be recorded between three points by adjusting valves, one pressure node is in the supernatant above the filter, the other right before the Triton® bottoms and the last one in the effluent piping. There is an additional pump for backwash water and there is also an air blower for air scouring. Backwash water is routed back to the flow channel via the overflow channel.

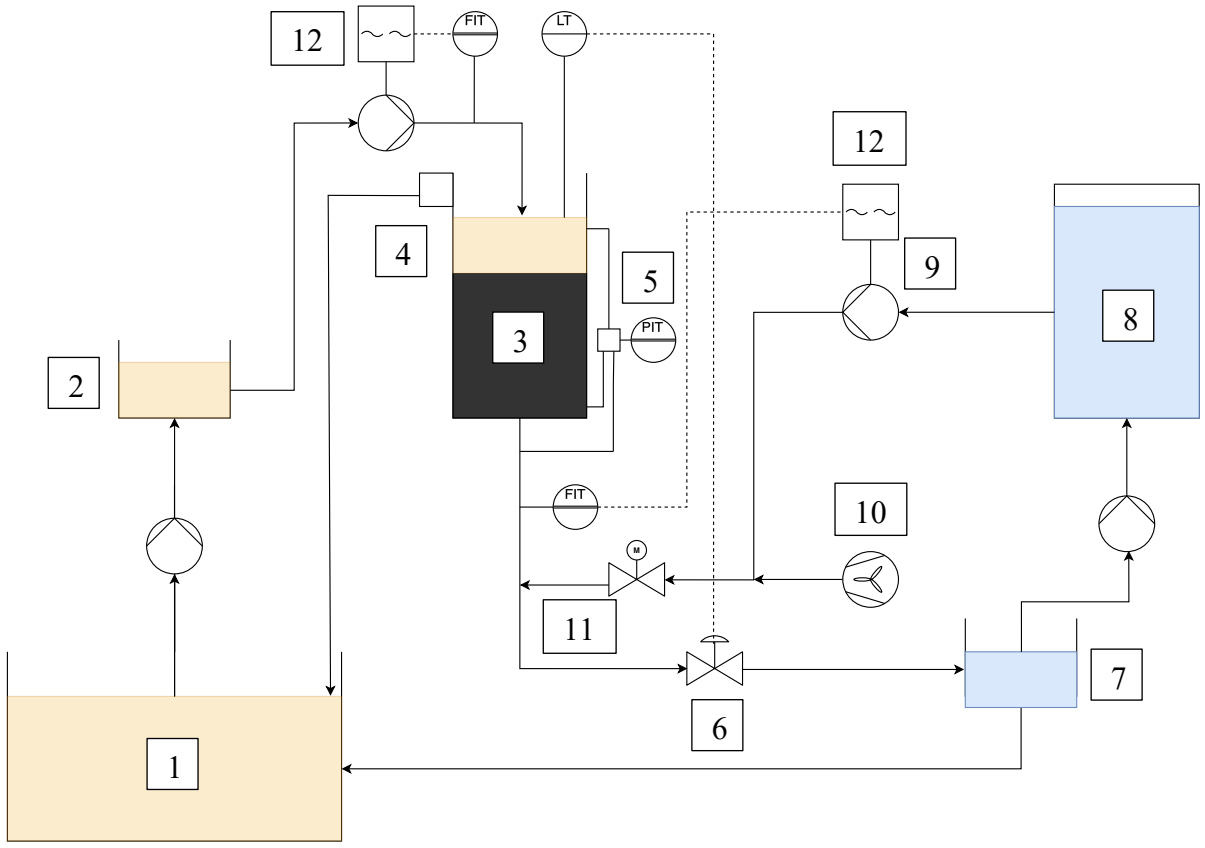

Figure 3.2: Simplified process flow diagram. The numbers correspond to: 1 (flow channel post disc filters), 2 (influent IBC tank), 3 (GAC pilot), 4 (overflow), 5 (pressure sensor), 6 (control valve), 7 (effluent tank), 8 (backwash water tank), 9 (backwash pump), 10 (blower for air scouring), 11 (electronic valve) and 12 (flow sensors).

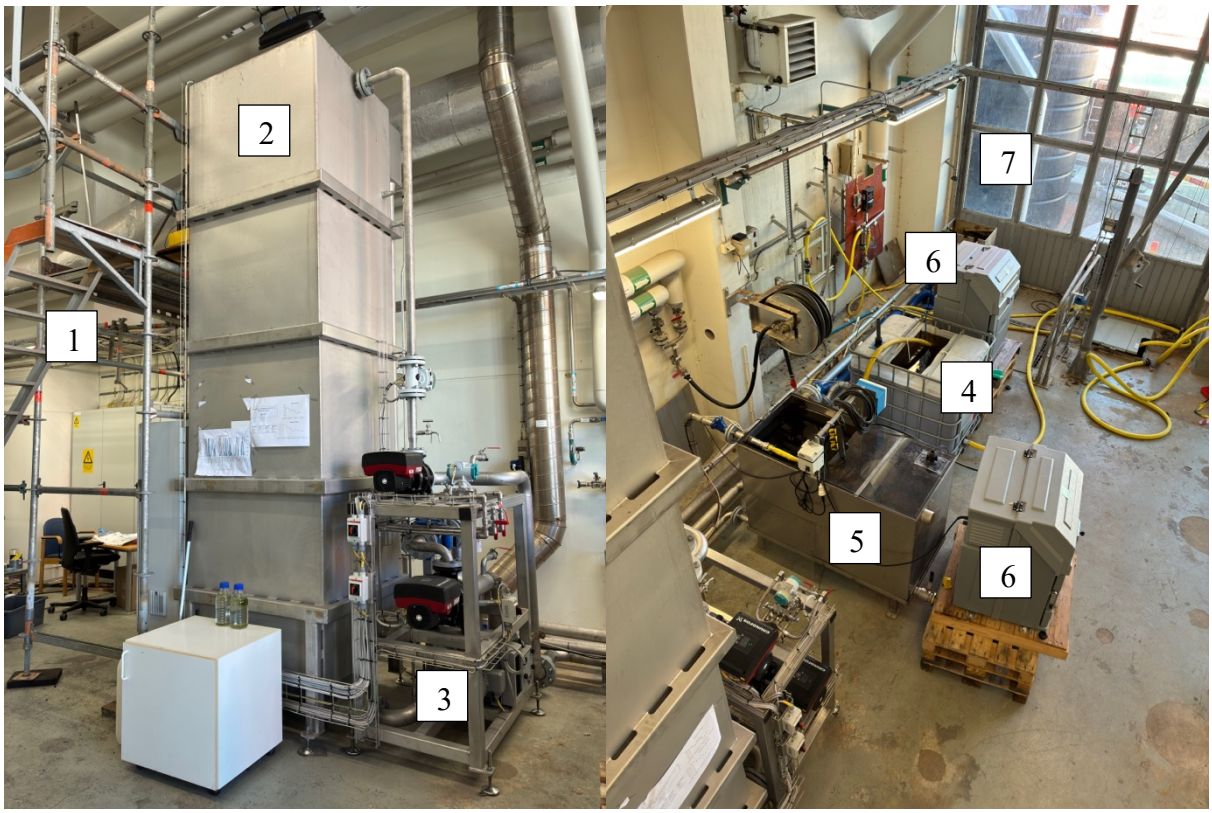

Figure 3.3. The numbers correspond to: 1 (scaffold), 2 (GAC pilot), 3 (instrumentation and control setup), 4 (influent tank), 5 (effluent tank), 6 (autosamplers) and 7 (backwash water tank).

Both influent and effluent tanks have turbidity sensors measuring online TSS concentrations, although it was installed and taken into operation during the spring of 2026. Each tank is equipped with autosamplers, see Figure 3.4. The top of the can be accessed via a scaffold in Figure 3.3. The water from the influent tank is fed to the open top centre of the GAC bed. There is also a water height sensor. The overflow channel running along the entire length of one of the sides can also be seen in Figure 3.5.

Figure 3.4. The numbers correspond to: 1 (influent tank), 2 (effluent tank), 3 (autosamplers), 4 (turbidity sensors).

Figure 3.5. Pictures showing the top of the GAC. The numbers correspond to: 1 (influent pipe), 2 (overflow channel) and 3 (water level sensor).

The GAC control software allows for backwashing to be triggered by timed intervals, totaliser setpoint and/or a selected combination of water level and valve opening. The backwash program has four sequences, see Table 3.3, where the first is an air-only sequence at a certain intensity in percent for a set duration. The second is an air-water-mix for a set duration and intensity for air and water respectively. Lastly, two consecutive water-only sequences that can be individually set to a desired duration and flow rate. In addition, the water level can be adjusted

prior to backwashing starts and pauses can be programmed between each sequence. The criteria for triggering the backwash program were 100% valve opening in conjunction with an increase in the water height to a certain level for 1 minute.

Table 3.3. Summary of the main sequences in a backwash program and how respective parameters could be selected.

Sequence	Parameter selection
Air	Intensity (%) and duration (s)
Air & water mix	Intensity (%) and duration (s)
Water 1	Flow rate (m^3/h) and duration (s)
Water 2	Flow rate (m^3/h) and duration (s)

3.2 Collection and Analysis of Project Operations Data

Data analysis was done in Python and Microsoft Excel, utilising pandas for data handling, *Matplotlib* for visualisation and *scipy* and *numpy* for numerical operations. From startup, data from the GAC filter was collected every minute including flow rates, pressure, water level, a number signifying the current step of the filter cycle and stored in a file. Influent and effluent TSS (from February) along with influent TSS in the flow channel was also collected every minute and archived separately. Thus, the TSS data had to be retrieved and merged with the GAC filter data log afterwards. However, for computational efficiency, TSS data was retrieved in 10-minute increments and assumed constant for each 10-minute period prior to merging.

A complete cycle consists of different steps each designated by a number. The starting point for each new cycle is defined by the first instance of a specific step (2). To distinguish between the cycles, each one was assigned an ID corresponding to the date and time of that starting step. To calculate cumulative bed volumes, filter run times and TSS load per run as well as the mean TSS concentration during a run, only the rows that include the production step (2) was used for each filter cycle.

Different water level criteria have been used to trigger backwashing and those triggered manually or automatically cannot be differentiated. Therefore, to assess filter run times and achieved TSS loads for complete runs only runs assumed to exhaust the max hydraulic capacity were selected. The chosen criteria were those runs that reached at least 0.25 bar in pressure loss and had longer filter run times than 30 minutes. In addition, for a few additional runs the flow channel TSS turbidity sensors max out and were therefore removed as the real values could not be accounted for. To find the initial pressure during a run, the average value between 5 and 20 minutes into a run was used to give time for process stabilisation.

3.3 Internal and External Lab Analysis of Standard Parameters & MPs

Certain standard parameters are analysed by the internal accredited lab at Gryaab. Every week, for both the GAC influent and effluent, 48h time-composite samples were prepared by auto-samplers. These samples were then analysed for total suspended solids (TSS), DOC (dissolved organic carbon) and UVA_{254} (ultra-violet absorption at 254 nm). Every month, there was also an extended analysis of additional parameters including BOD (biological oxygen demand), COD, TOC, P_{tot}, N_{tot}, NH_4-N, NO_3-N, NO_2-N and PO_4-P.

The following analytical methods were used for the standard parameters:

- TSS with a method based on SS-EN 872:2005.
- N_{tot}, TOC and DOC were analysed using a Formacs Combustion TOC analyser.
- BOD (LCK554) and COD (APC314) were analysed spectrophotometrically with Hach-cuvettes.
- NH_4-N, PO_4-P, NO_2-N, NO_3-N were analysed spectrophotometrically on a SEAL Analytical AQ400 Discrete Analyzer
- UVA_{254} and P_{tot} were analysed with a Hach DR6000 using a modified method based on SS-EN ISO 6878:2005.

Analysis of micropollutants was conducted externally at MoLab (Kristianstad). For more information see (Svahn & Björklund, 2016; Svahn & Björklund 2019). Analysis of PFAS-24 was instead done externally by SGS.

3.4 Suspended Solids Mass Balances

To be able to assess the performance of the backwashing programs, the influent and effluent TSS (installed February of 2026) concentrations were continuously monitored with online turbidity sensors from Endress+Hauser. There was an additional turbidity sensor in the flow channel from which water to the IBC was pumped. Based on this data, the total TSS load and the TSS retained by the GAC filter during a filter run could be approximated by the trapezoidal rule under the assumption of constant TSS concentration for each 10-minute segment.

To measure the concentration of TSS in the backwashing water, time-composite sampling with aliquots of 100 ml per minute was drawn from the overflow. To be able to investigate changes in TSS concentration with time during a backflush program, samples were collected separately every minute. Validation of the turbidity sensors was done by collecting samples from the influent IBC and effluent tank in 10 L containers and recording the displayed concentrations and time.

Whatman GF/A filters with a 1.2 μm pore size were used for filtration. A random selection of filters from each factory new box had been tested for loss in filter mass according to SS-EN 872:2005. The filters were dried in an oven for 1 h at 105°C followed by cooling in a desiccator for 30 min both before and after filtration to account for varying environmental conditions. Prior to filtration, each sample was thoroughly shaken, to limit sedimentation and the resulting volume was recorded. Once the sample had been successfully filtered, the cylinder and funnel were cleansed with distilled water. Samples taking longer than 10 min to filter were rerun and residues under 2 mg should be interpreted with caution.

3.5 GAC collection procedure

Tubing from a peristatic pump was fastened to a 3 m telescoping metal rod with a plastic square jar (1000 ml) fitted tube connectors to act as the GAC collection bin, see Figure 3.6. The rod was marked with the desired depths. Samples were collected at 30% bed expansion. To collect GAC, the rod was lowered to a certain depth whilst pumping in reverse to prevent granules from entering the collection jar. Next, the pump was turned on and an appropriate amount of GAC was collected and was transferred to separate jars.

Figure 3.6. The jar used for collecting GAC at different depths into the expanded bed.

3.6 Mini GAC Column to Assess Hydraulic Capacity

To assess the hydraulic capacity of the GAC a set-up was constructed out of two Fisher 50 ml centrifuge tubes, a metal mesh, some tubing, tube adapters and a peristatic pump. The rationale was to measure the head that was needed to drive a constant flow through a certain GAC bed height to see relative changes in hydraulic capacity between new GAC and GAC from different depths in the expanded bed.

A hole was drilled at the bottom of a centrifuge tube to which tubing was glued, see Figure 3.6. A tube adapter was connected at the end of it. This tube adapter served as the water outlet or by connecting the inlet tube to the tube adapter, water could be pumped in the opposite direction to simulate backwashing. A metal mesh was inserted to the centrifuge tube to keep the GAC particles from escaping. An additional centrifuge tube was used to accommodate large water heads. The entire set-up can be seen in Figure 3.7.

To operate the small-scale GAC filter in close to the same operational regime as the GAC filter, the filter velocities were approximately matched (0.208 cm/s). Using the top inner diameter of 2.72 cm of the centrifuge tube the desired flow rate for the peristaltic pump was ~73 ml/min. To maintain close to constant flow rate, the temperature of the water in the water reservoir was collected from the faucet at the same setting (7-13°C).

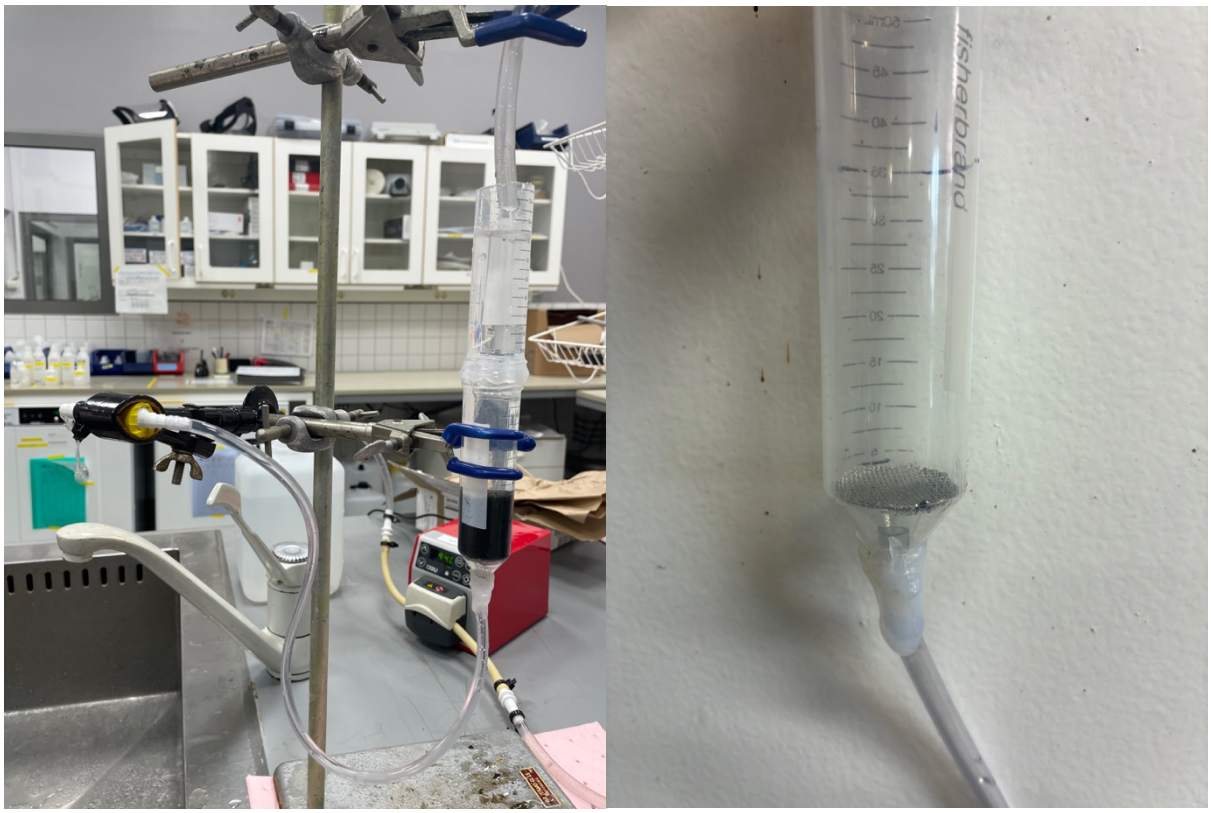

Figure 3.7. The set-up for the mini-column tests and close-up of the column.

To account for the resistance of the centrifuge tubes, the metal mesh and the tubing, the set-up was allowed to run with only water. Once the head had stabilised at the desired flow rate was reached, the head was measured from the same reference point, h_{ref}. Next, GAC was transferred to the centrifuge tube and was backwashed for 2 minutes at max flow rate to remove residual TSS in the water left from collection. After backwashing, the column was fed with the desired flow rate and the stabilised water head and bed height (L) was measured, h_{GAC}. Repeated twice thereafter, the GAC was backwashed for 30 seconds to re-stratify the bed and h_{GAC} was measured. Altogether producing three recordings of h_{GAC} for each GAC sample. The head and corresponding pressure drop required to maintain constant flow becomes

$$\Delta h = h_{GAC} - h_{ref}$$

$$\Delta p = \rho g \Delta h$$

From these equations and by knowledge of the bed height, L, the pressure drop per meter bed could be calculated according to

$$\Delta p \text{ per meter bed (mbar/m)} = \frac{\Delta p}{L}$$

The set-up was run with new GAC to verify that wall-effects or other factors had minimal effect on the results. New GAC was backwashed for 4 minutes to remove fines.

The three measured values used in the calculations each had an estimated instrumental uncertainty of ± 1 mm. This was done as a measure to account for alignment issues, despite the measuring device technically permitting finer readability (± 0.5 mm). The instrumental uncertainties were propagated through the calculations. Reported uncertainties combine the measurement uncertainties as standard deviation of the technical replicates and the average propagated instrumental errors per depth with the root-sum-square method.

3.7 Particle Size Distribution Analysis

To characterise how the GAC particles are stratified in the bed, a dry sieving was done to assess the particle size distribution (PSD) based on mass for GAC at different depths and new GAC as a reference. Dry sieving was chosen over wet sieving for efficiency as the GAC could be dried before sieving rather than drying individual fractions after sieving. To remove residual TSS from GAC collection, GAC was carefully mixed with tap water and the supernatant decanted. The GAC was then transferred into aluminium trays and dried overnight in an oven at 105°C. A bottom catch container along with sieves at 0.2, 0.4, 0.6, 1.0, 1.4, 2.0 mm were used. The sample mass was in the range 10-20 g. Each sample was placed at the top sieve and then put into an autosiever for 10 minutes. The autosieve had a singular marked speed used for all samples. Once finished, the individual fractions were transferred onto aluminum foil and a brush was used to clear the sieves of any stuck particles followed by recording the weight using an analytical balance. It was assumed that moisture absorption by the biofilm was negligible and equally absorbed across the different depths. To verify this, some of the GAC samples were dried in an oven at 105°C for 2 h after sieving and then weighed for comparison.

3.8 Microscopy

An Olympus BX53 microscope was used to investigate the presence of biofilm growth on the GAC particles. Images could be taken by the internal software and 16x-40x magnification was used. The software allowed for measurements of the grain size and biofilm thickness.

3.9 Dissolved Oxygen and Sub-atmospheric Pressures

Dissolved oxygen (DO) measurements have been occasionally measured with a DO probe in the influent and effluent tanks to investigate if it changed during filter runs. To track sub-atmospheric pressure development at a certain depth an elementary pressure apparatus (metal rod equipped with manometers) was inserted 50 cm into the bed and the values recorded every 15 minutes during a filter run.

4 Results & Discussion

The results will be divided into operational results and treatment related results. The former covers operational aspect of the GAC filter, e.g. evolution of filter run times, TSS load per run and biofilm growth and the latter how the GAC pilot has treated the substances from the revised UWWTD, standard parameters and PFAS-24.

4.1 Operational Results & Discussion

An overview will first be given of the entire operational history of the GAC pilot followed by more in-depth review of the evolution of filter run time, TSS load per run, TSS influent concentration, biofilm growth, pressure drop curves and initial pressure.

4.1.1 Overview of Operational History

Figure 4.1 shows an overview of the entire operational history GAC pilot, where the treated bed volumes are plotted versus time from commissioning in July 2025 until May 11, 2026 (~14,300 BV). This time period has been divided into different subperiods, the startup and baseline operation phase, from commissioning until about midway through October, which is followed by a progressive deterioration in the operational aspects of the filter that lasts until the remediation phase in late March of 2026, which involved lowering the bed height (~11,300 BVs). There are also two periods of operational downtime in November and January.

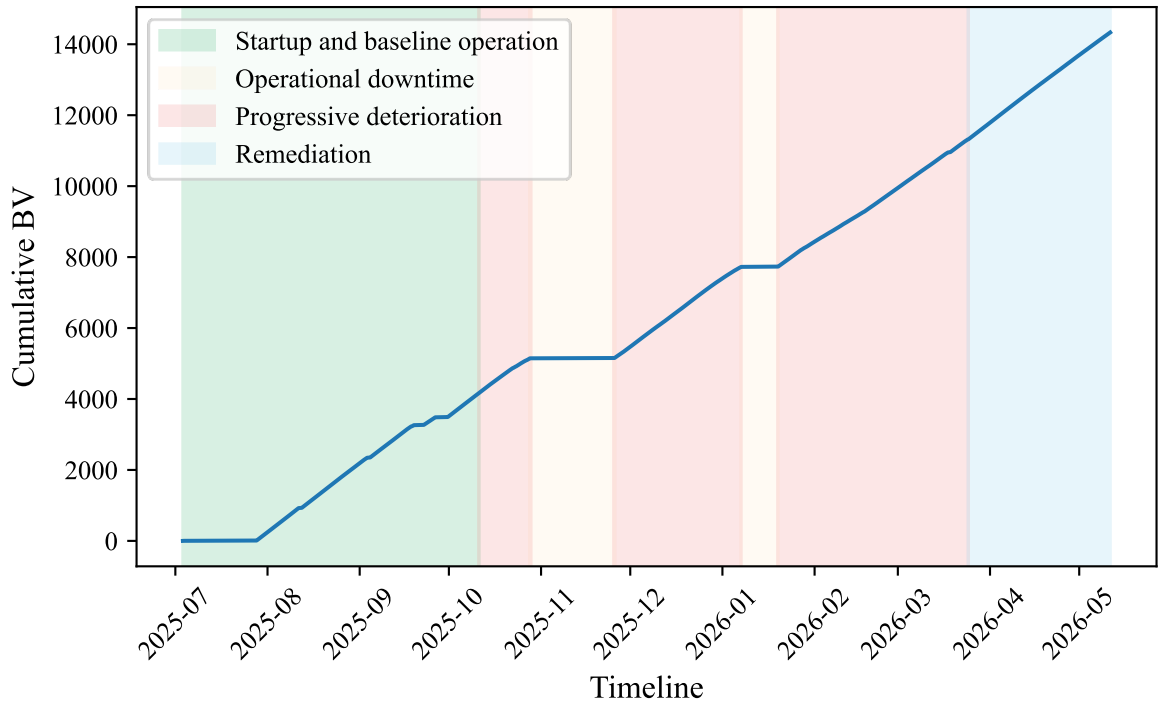

Figure 4.1. Plot showing the operational history of the GAC pilot as the cumulative bed volumes over time.

A total of 1,106 filter cycles have been run. Based on the filter criteria for a complete cycle as described in the methods section, 949 were successful in reaching 0.250 bar and 30 minutes of filter run time. Except for four filter runs, the remaining reached a pressure drop between 0.250-0.282 bar.

Evolution of Filter Run Time and Solids Load

The filter run time and corresponding TSS load per run can be seen for the operational history of the GAC pilot in Figure 4.2. The startup and baseline operation phase from commissioning in June until almost midway through October 2025 has a fluctuating filter run time and TSS load per run with a mean of 12.3 ± 5.9 h and 270 ± 118 g TSS respectively. The start of this deterioration phase leads up to the first period of operational downtime in late October 2025 and lasts until late March 2025. During this period both the filter run time and TSS load per run had decreased, with means of 3.0 ± 2.2 h and 96 ± 92 g TSS respectively, but as low as 1.5 ± 0.4 h and 37 ± 13 g TSS for the worst sustained period (2026-01-27 to 2026-02-17). Large variations in solids load per run have been reported elsewhere (Schölzel et al., 2022).

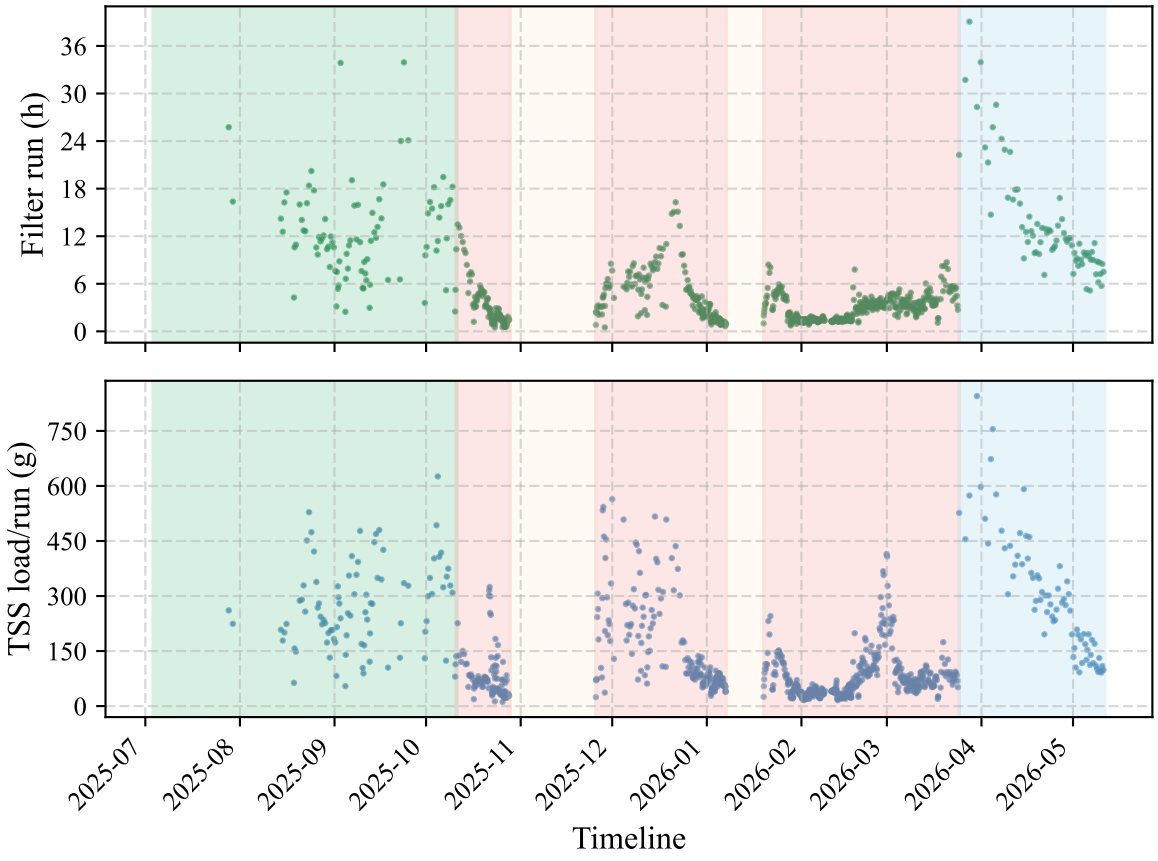

Figure 4.2. Plot of the filter run time and solids load per run for the entire operational history of the GAC pilot.

The first operational downtime was caused by an infestation of bell-shaped ciliates, Vorticella, in the disc filters in conjunction with shortage of sodium hypochlorite for cleaning, leading to

the GAC pilot being taken offline until late November. In the ensuing period until the second operational downtime, the GAC pilot first saw an improvement with respect to filter run time and TSS load per run, which then regressed toward the end of December 2025 leading up to the second operational downtime in the beginning of January. In the subsequent period, the GAC filter exhibited fluctuations in the filter run time and TSS load per run, but they remained altogether consistently worse than during the startup and baseline operation phase. The short filter run times necessitated frequent backwashing several times per day. As the backwashing program uses the effluent during the water phases, significant amounts of the treated water was used to clean the GAC pilot itself, which prevented economical operation. In addition, the frequent backwashing also meant some of the water was treated more than once, which could skew the adsorptive performance results. Following troubleshooting, the bed depth was decreased which improved both the filter run time and TSS load per run, see Chapter 4.1.4 for more information.

From design guidelines found in literature it is recommended to design for at least 24 h of operation before backwashing. With a GAC particle size interval of 0.6-2.4 mm, an influent TSS concentration below 5 mg/L and an available water head of 3-4 m, the achievable TSS load should be at least 500 g TSS/m^2 filter in 85% of filter runs (Böhler et al., 2023). In comparison to the GAC pilot at Rya WWTP, the TSS load achieved in 85% of filter runs during the startup and baseline operation and deterioration phases was at least 137 g TSS/m^2 and 30 g TSS/m^2 respectively. This was with a mean influent concentration during the entire operational period of the GAC pilot of 4.1 mg/L, see Chapter 4.2.1. The driving force was between 0.25-0.28 bar, or about 2.5-2.8 m. However, when the GAC pilot was idle, there was a static zero offset (no flow) of 0.05 bar, which renders an effective driving force of 2-2.3 m. In addition, the particle size interval was 0.425-2.36 mm, which is smaller than the stated interval from design guidelines. With these differences in consideration, for most filter runs, a TSS load less than 500 g TSS/m^2 filter can be expected before backwashing is triggered.

Evolution of Pressure Curves and Initial Pressure Loss

Figure 4.3 shows examples of the pressure drop curve for selected filter runs from different operational periods.

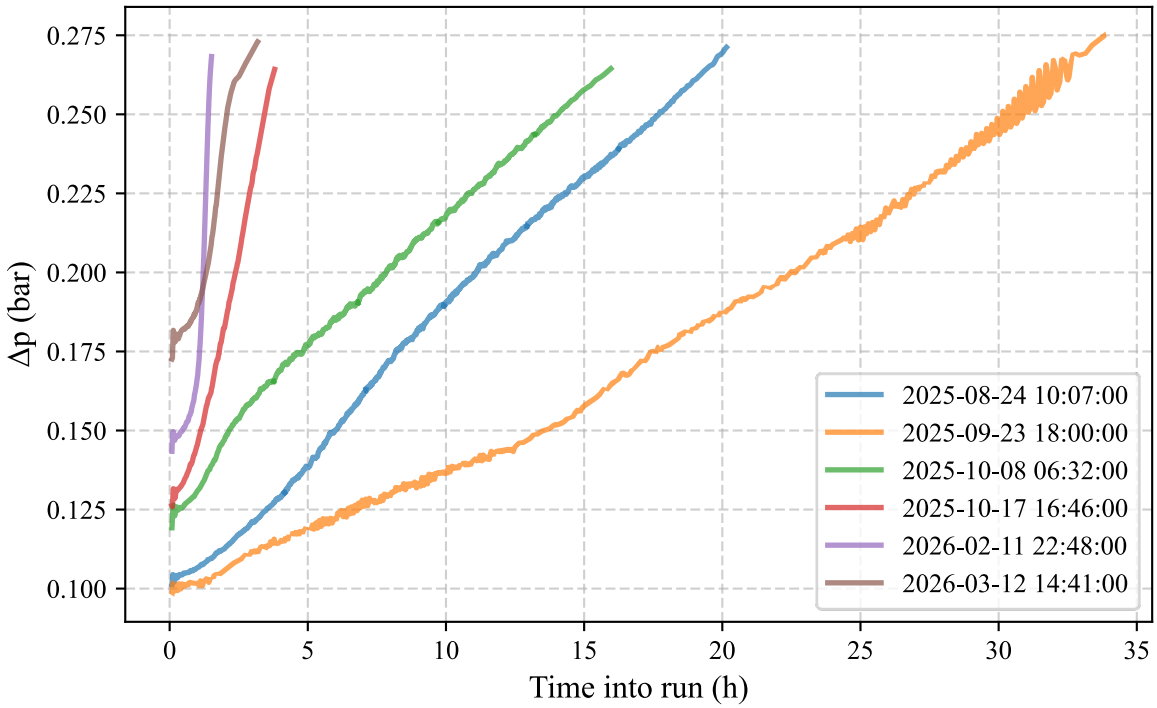

Figure 4.3. The pressure drop curve for selected filter runs throughout the operational history of the GAC pilot.

In the examples from the startup and baseline operation phase (orange, blue and green), the pressure drop increases more slowly, which indicates solids retention deeper into the bed (Schölzel et al., 2022). However, starting in October at the onset of the deterioration phase (red), the pressure drop becomes increasingly more rapid toward February and March. This indicates more of a surface filtration effect, which means solids are being primarily retained at the top of the bed (Schölzel et al., 2022). In addition, the initial pressure increases with time, from ~0.100 bar in the startup and baseline operation phase to ~0.175 bar in March. Consequently, reducing the available driving force during filter runs. See Chapter 4.1.4 for a closer look at the period after remediation.

Influence of Temperature on the Initial Pressure Drop

It was investigated whether the high initial pressure drop exhibited before the lowering of the bed could be explained by temperature changes alone since colder water temperature increases the resistance of the bed based on the numbers given by the manufacturer. It was assumed the initial pressure drop is the pressure drop when the influent and effluent flows have stabilised. For several filter runs in March the water temperature was about 10°C with an initial pressure drop of ca 0.17 bar. Contributing to this initial pressure drop was the static zero offset (no flow) of 0.05 bar and the pressure drop across a 2.7 m bed of 0.06 bar based on the numbers from the manufacturer at 10°C. However, there is still around 0.06 bar of pressure drop unaccounted for, which points to additional factors like biomass growth may be contributing to the higher initial pressure drop compared to the startup and baseline operation phase.

Correlation Between TSS Concentration and Filter Run Time

The mean incoming TSS concentration per run was plotted versus the filter run time to investigate if changes in the feed quality could have an impact on the filter run time and if this correlation changes for different periods of the operational history. Figure 4.4 shows six periods, the startup and baseline operation phase, different parts of the deterioration phase, the worst sustained operational period and after the lowering of the bed.

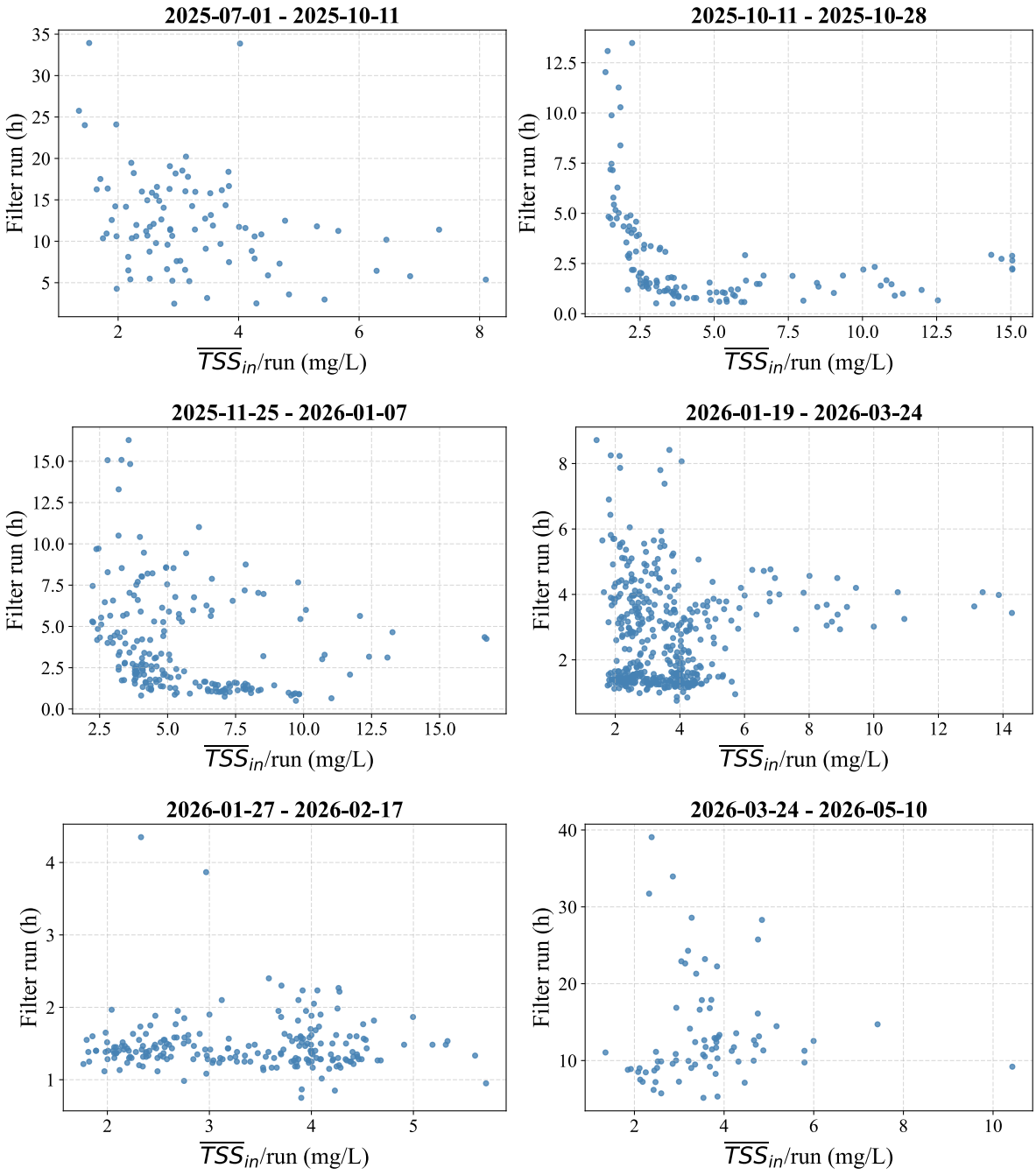

Figure 4.4: Filter run time plotted versus mean influent TSS concentration for different periods of the operational history of the GAC pilot.

Spearman rank correlation tests were conducted for each period to evaluate the relationship. During the startup and baseline period (2025-07-01 to 2025-10-11), there was a statistically significant weak negative correlation (r_s = -0.31, p = 0.003, n = 90). For the first part of the deterioration phase (2025-10-11 to 2025-10-28), there was a statistically significant moderate negative correlation *(*r_s = -0.64, p < 0.001, n = 121). After the first operational downtime the period (2025-11-25 to 2026-01-07), also exhibited a statistically significant weak correlation (r_s = -0.42, p < 0.001, n = 198). However, the period after the second operational downtime to the bed lowering (2026-01-19 to 2026-03-24) exhibited no statistically significant relationship (r = - 0.02, p = 0.705, n = 451) and investigating the congested lower left corner of this period (2026-01-27 to 2026-02-17) this was also not the case (r_s = - 0.02, p = 0.723, n = 213). For the entire period following bed lowering (2026-03-24 to 2026-05-10), there was instead a positive significant correlation between the filter run time and mean influent TSS concentration (r_s = 0.28, p = 0.014, n = 75).

Altogether, the mean influent TSS concentration has limited explanatory power for the shorter filter run times. Initially, a statistically significant weak correlation was exhibited, which shifted to a negligible correlation for the worst performing period. This indicates that the correlation varies with time due to changing conditions. One important factor could be prominent biofilm growth, which may become the predominant factor over TSS in causing significant hydraulic resistance and thus a clear relationship is not always observed (Schölzel et al., 2022).

To determine the suitability of a GAC filter, during the planning stage, it has been recommended to investigate the TSS load during 24 h based on the influent TSS concentration (Schölzel et al., 2022). With the average influent TSS concentration of 4.1 mg/L from Chapter 4.2.1, the TSS load is about 0.74 kg/24 h/m^2 filter based on a flow rate of 7.5 m^3/h. Because this value is significantly below 2.3 kg/24 h/m^2, it should theoretically be possible to operate the filter for 24 hours before backwashing under normal operation, otherwise pretreatment is recommended. Although, this value is based on a GAC grain size of 0.63-2.36 mm, which is greater than what is used in the GAC pilot, the influent TSS concentration by itself appears to not be high enough to necessarily warrant pretreatment.

4.1.2 Signs of Biofilm Growth

Biofilm growth could be noted in the influent IBC and around the interior of the GAC pilot, see Figure 4.5. Despite repeated cleaning attempts of the influent IBC and interior of the GAC pilot, growth shortly reappeared in all vessels both before and after the bed was lowered.

Figure 4.5. Pictures showing biofilm growth in the interior of the GAC filter and the influent IBC tank.

In addition, the GAC particles at the top layers before bed lowering exhibited a brownish coating in comparison to new GAC. To investigate differences in biofilm growth on the particles, GAC was collected from different depths and then viewed through a microscope. Figure 4.6 shows images taken of GAC particles from different depths into the expanded bed.

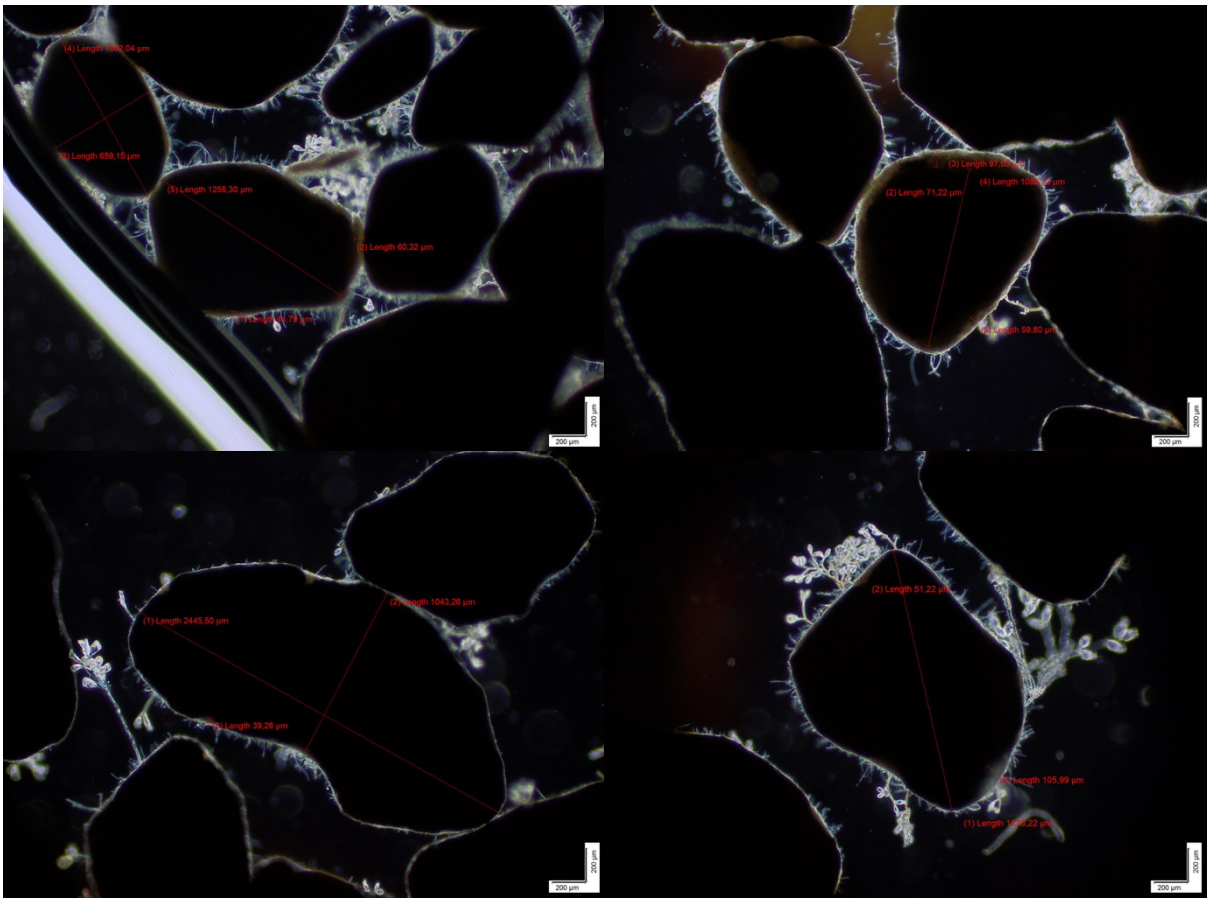

Figure 4.6: GAC particles from different depths into the expanded bed viewed in a microscope. From above going left to right: 20 cm, 220 cm, 120 cm, 170 cm. The red text shows dimensions of certain particles as well as of the extent of biofilm growth.

Upon inspection, biofilm growth can be confirmed by varying degree and coverage on the GAC particles, in some cases more than 100 µm. However, the biofilm growth showed no decisive preference for certain GAC sizes and there were no clear nor consistent differences in coverage between depths.

Both before and following the lowering of the bed height, the DO concentration was measured on separate occasions in the influent and effluent tank. From these measurements, the water entered almost saturated with oxygen, but left effectively devout of it. As an example, the DO concentration was measured throughout a complete 270-minute cycle before the bed was lowered, the water in the influent IBC measured 10.08 ± 0.15 mg O_2/L and the effluent, 0.29 ± 0.02 mg O_2/L, throughout the filter run. This removal of DO can likely be attributed to biofilm growth or sub-atmospheric pressure formation in the bed. From Chapter 4.2.1, BOD removal was confirmed and nitrification suggested, which consume DO. This indicates the decrease in DO could be attributed to biofilm growth (Fundneider et al., 2021b). However, during this filter run the local pressure equalled the pressure drop for the last 30 minutes of the run. In addition, bubble formation was confirmed in the bed upon poking the surface (has been observed during other filter runs). This could indicate formation of local sub-atmospheric pressures in the bed, which can cause dissolved gases to escape form the water. This has been observed in other

downflow GAC filters when they are allowed to exhaust their hydraulic capacity and can result in hydraulic blockage and worsened adsorptive performance as it reduces the effective filter cross sectional area due to bubble entrapment (Schölzel et al., 2022). However, as the difference in DO in the influent and effluent is relatively constant throughout the filter run, this suggests biofilm growth is more likely.

4.1.3 Localisation of Hydraulic Resistance in the Bed

To be able to localise and estimate the hydraulic resistance at different bed depths, the mini-column test according to Chapter 3.5 was developed with GAC collected at different depths. Mini-column tests were then run and the corresponding data can be found in Table A. The pressure drop per meter bed could be calculated and the corresponding pressure profile constructed, see Figure 4.7. For verification of method, see Table A2.

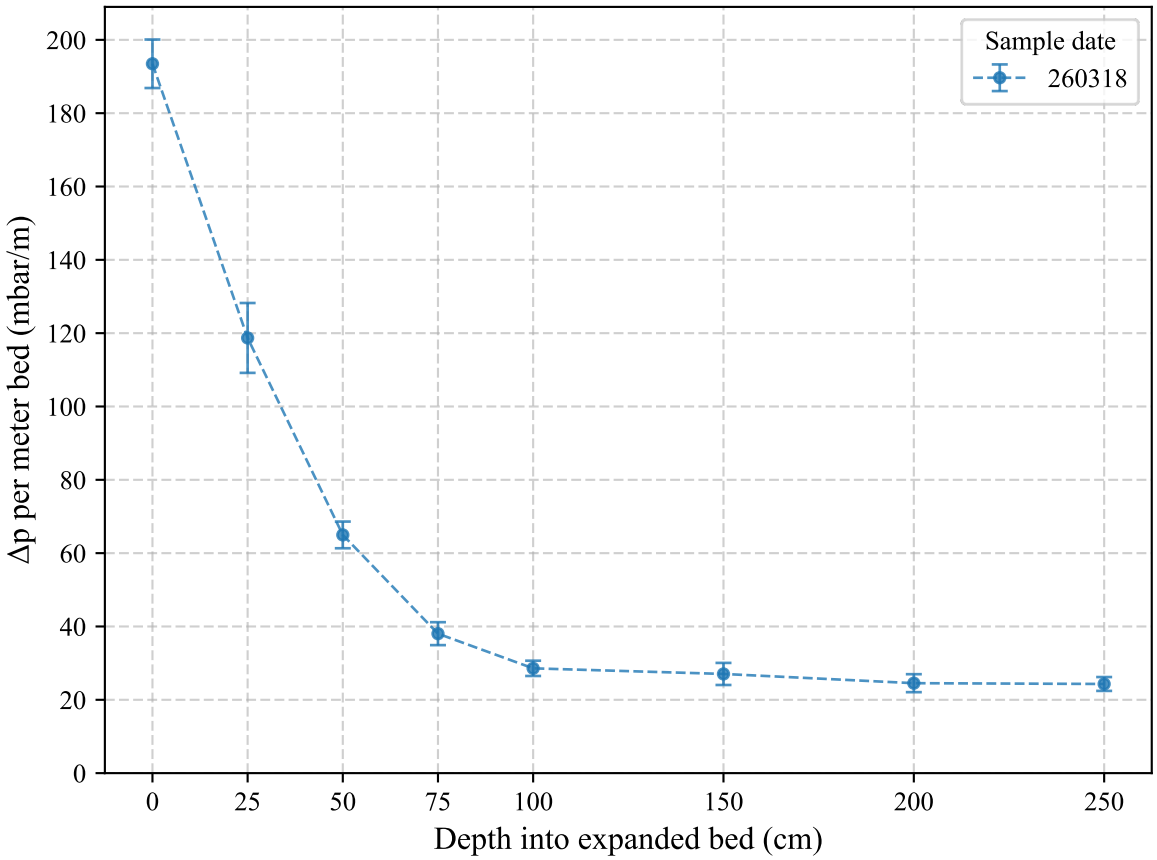

Figure 4.7. Pressure profile as the pressure drop per meter bed (mbar/m) for GAC collected at different expanded bed depths.

The top layers of the expanded bed, from 0-50 cm appears to produce significantly more hydraulic resistance than the rest of the expanded bed, which exhibits small differences between the depths. Thus, the major hydraulic resistance was localised to the top part of the bed, which was expected based on the appearance of the pressure drop curves and unaccounted for initial pressure drops.

A PSD test (Table B1) of the GAC at depths of 0 cm, 50cm, 100 cm and 250 cm into the expanded bed was conducted to investigate bed stratification, see Figure 4.8. The PSD test for new GAC (Table B2) as a reference can also be seen at the bottom of the figure. Verification of this method can be found in Table B3.

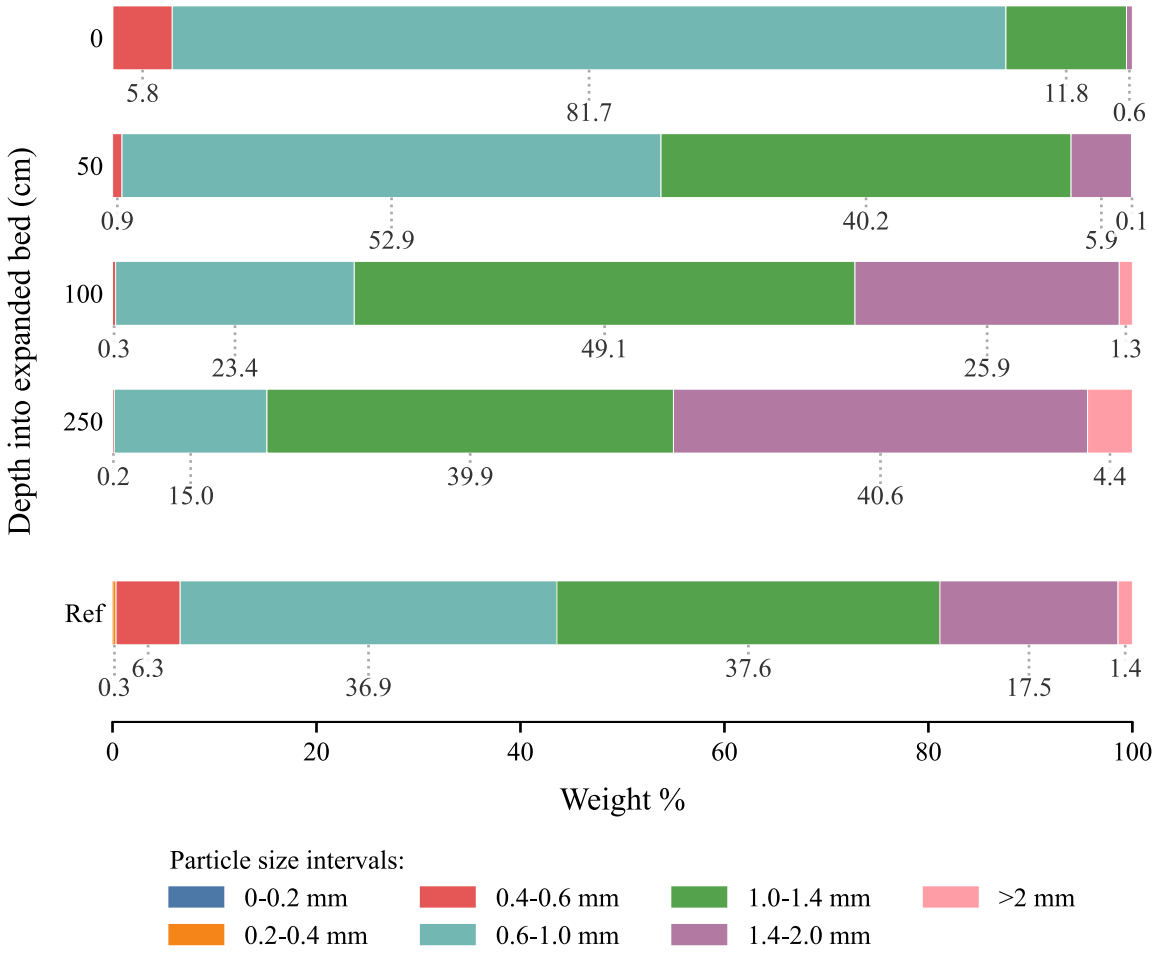

Figure 4.8. Particle size distributions (PSDs) for GAC collected at different depths into the expanded bed and the PSD for new GAC as reference before the bed height was lowered.

Comparing the PSDs for different depths, there was a clear difference between them, with smaller particle size intervals being featured predominantly at the topmost layer of the bed and larger particle size intervals at the bottommost layer, with a corresponding decrease or increase depending on particle size in between the extreme layers. Comparing the results to new GAC confirmed that the bed had become stratified. In addition, the majority of particles for new GAC were in the intervals 0.6-1.4 mm, which was expected based on the specifications. Relating the PSD to the pressure profile appearance, the smaller grains at the top lead to greater local hydraulic resistance which supports the results from the mini-column tests. From literature this also means that the top layer of the bed could enhance the surface filtration effect and result in

a more rapid and non-linear increase in pressure drop during filter runs as seen in Chapter 4.1.2 (Schölzel et al., 2022).

4.1.4 Remediation Phase and Comparison

The localisation of the hydraulic resistance to the top layers of the bed in conjunction with the short filter run time prompted action to lower the bed height to see if it would improve the operational aspects. On March the 24th the bed was lowered to approximately 2.22 m and the EBCT was correspondingly decreased to match the previous EBCT under the assumption of a previous bed height of 2.7 m. The new filter velocity and flow became 6.16 m/h and 6.16 m^3/h respectively. Because of the proximity to the filter overflow before bed lowering, the GAC pilot was limited to approximately 20% bed expansion to prevent GAC washout during backwashing. The lowering of the bed increased this distance to ~1.33 m, which permitted more aggressive backwashing programs. This is in line with what has been recommended to prevent washout (minimum 1.2 m) ((Schölzel et al., 2022). The maximum bed expansion before bed lowering was on the lower edge of what has been suggested (25%) (Böhler et al., 2023), but more than 45% was now possible.

Filtration Run Time and Solids Load per Run

Figure 4.9 shows a comparison of the filter run time and TSS load per run for the period preceding bed lowering and the period immediately following bed lowering.

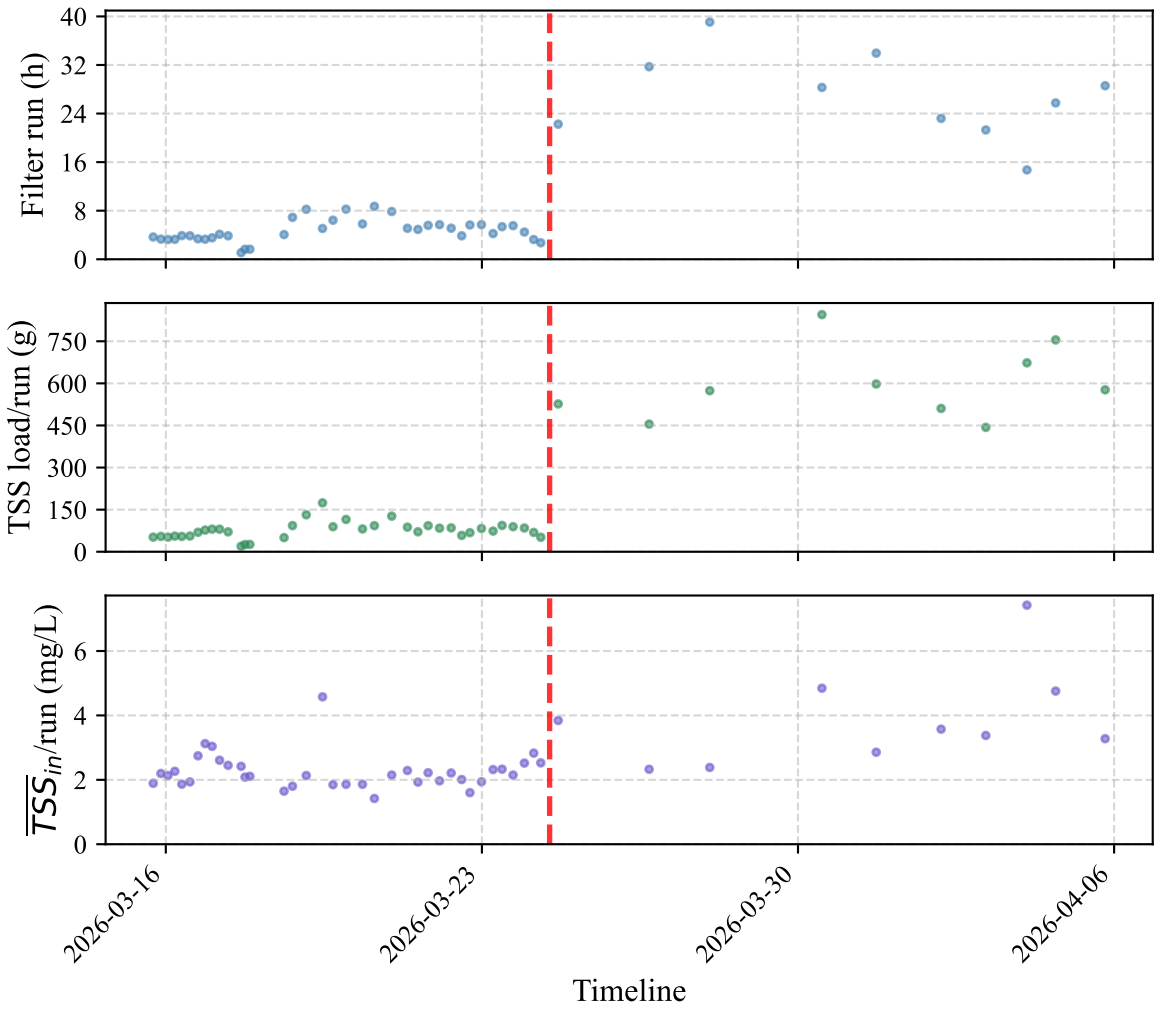

Figure 4.9. Plot of the filter run time, TSS load and mean influent TSS concentration per run before and immediately after the lowering of the bed. The vertical red line signifies the lowering of the bed.

The improvements can clearly be seen. The entire first three weeks following the change exhibited a mean filter run time of 24.0 ± 6.5 h and TSS load per run of 515 ± 139 g TSS at a similar mean influent TSS concentration per run. These weeks following the change in bed height is the best sustained operational period of the GAC pilot. However, the GAC pilot soon approached worse figures.

Following bed lowering there is largely an absence of the 0.4-0.6 mm particle size (see Evolution of Particle Size Distributions), this means the particle size interval is closer to 0.6-2.36 mm overall. The TSS load achieved in 85% of filter runs for the first three weeks was at least 395 g TSS/m^2 filter. This is almost in line with what can be expected for an available driving force of 3-4 m (Böhler et al., 2023), which is more than the 2-2.3 m in this GAC pilot.

In Figure 4.10 the entire remediation phase with respect to mean filter run time and TSS load per run can be seen.

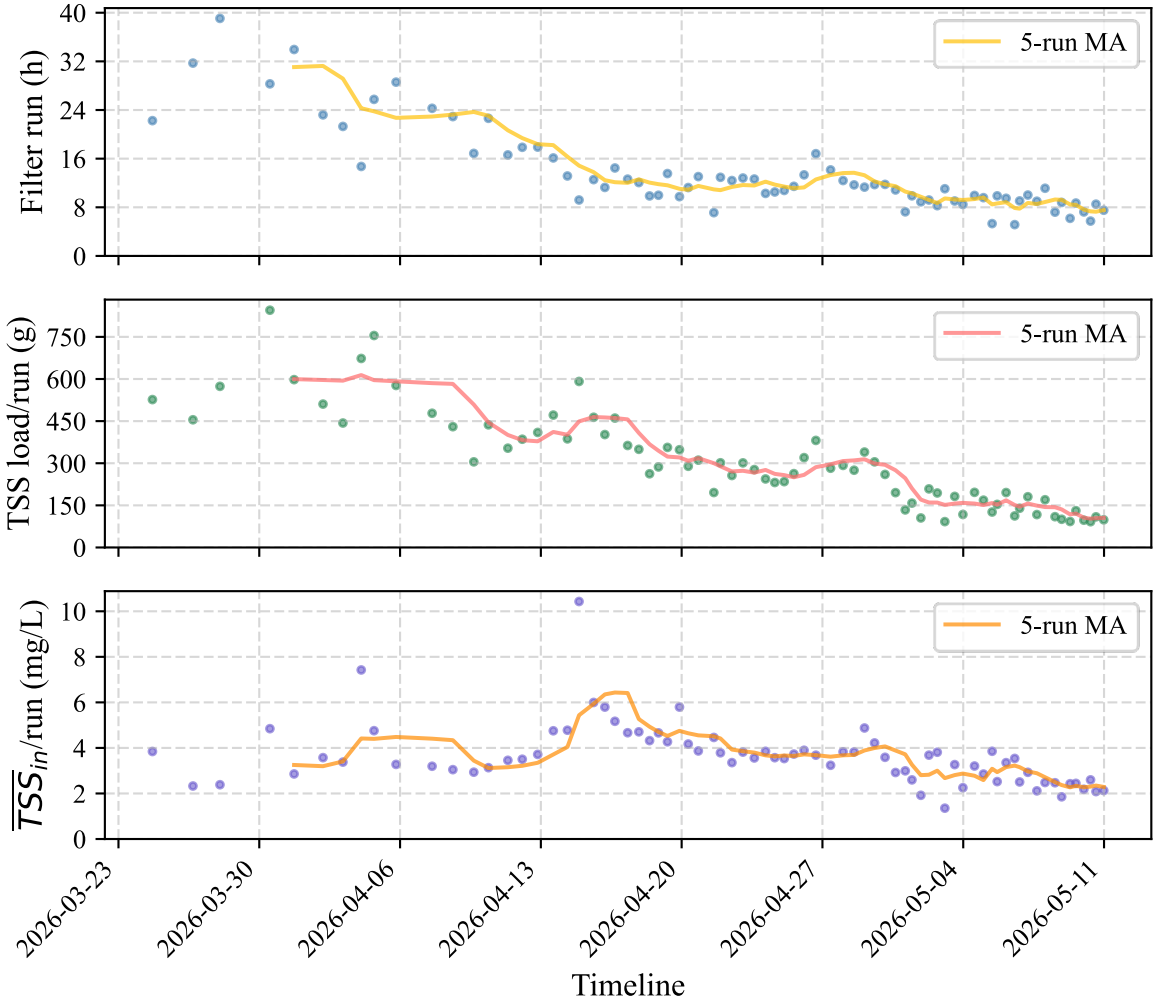

Figure 4.10. The filter run times, TSS per run and mean influent TSS per run and their respective moving average over five filter runs for the period after the bed was lowered.

Despite increased backwashing aggressivity in bed expansion and air scouring (see section on Backwashing below), after the first three weeks the filter run time and TSS load per run show a downward trend. For the entire remediation period, the filter run time has a mean of 13.5 ± 6.8 h and a TSS load per run of 302 ± 167 g TSS, which is similar to the startup and baseline operation phase, but still an improvement in comparison to the deterioration period. However, judging by the trend in May, the decrease in performance is expected to progress.

Evolution of Pressure buildup and Initial Pressure Drop

In Figure 4.11, the pressure buildup for selected filter runs during the remediation can be seen.

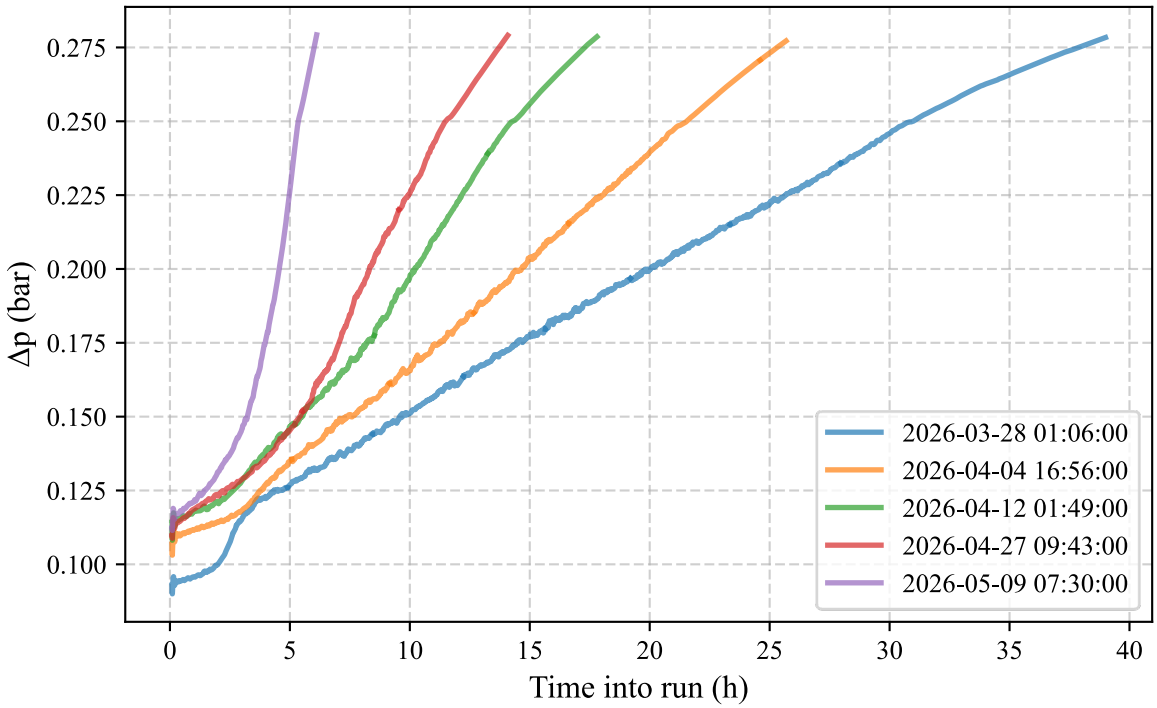

Figure 4.11. The pressure drop curves for a selection of filter runs following lowering of the bed plotted versus the time into each run.

Closely following the bed lowering, the pressure drop curve again increases more slowly, similarly to the startup and baseline operation phase. This is indicative of retention deeper in the bed, which is desired and despite the lower filtration rate compared to before bed lowering, which could lead to enhanced surface filtration. Later in April and May, the pressure drop curve increases more rapidly, resembling what is seen in the deterioration phase, which indicates more of a surface filtration effect. This is the same change in behaviour seen when comparing the startup and baseline operation phase to the deterioration phase before the bed was lowered.

In Figure 4.12 the initial pressure drop for the filter runs just before and after bed lowering can be seen.

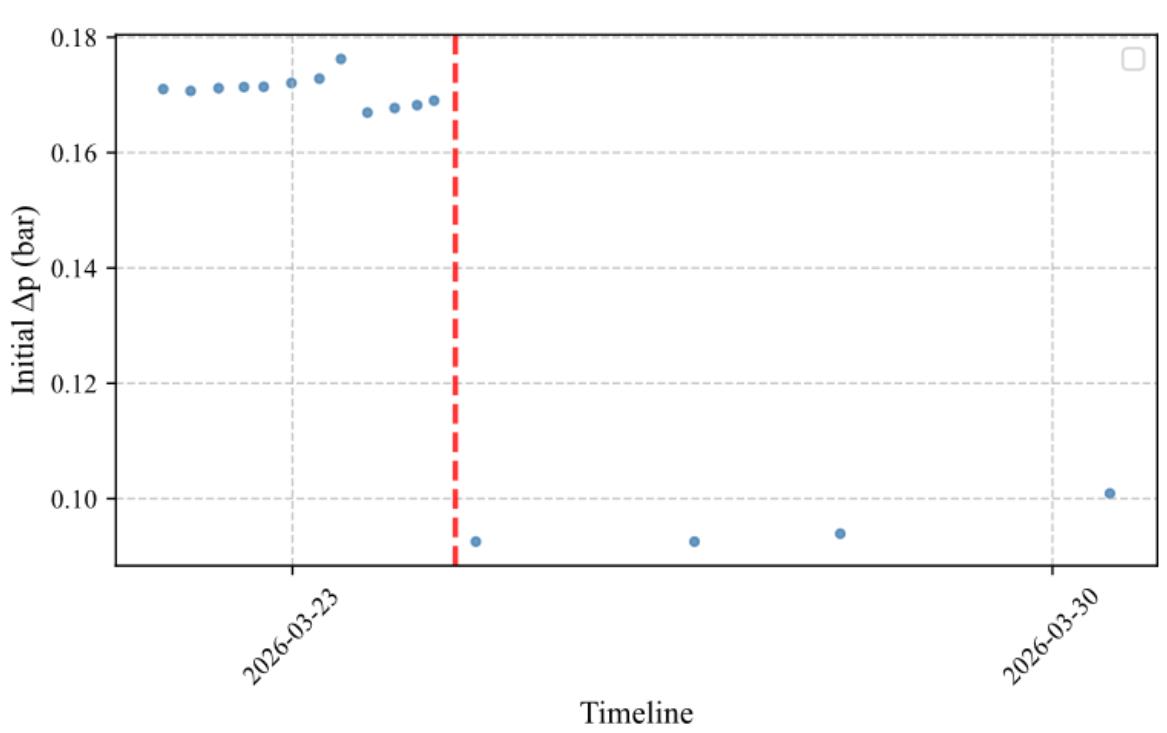

Figure 4.12. The change in initial pressure before and after lowering the bed height. The red line signifies the time of the change.

The initial pressure drop decreased considerably following bed lowering, down to about 0.925 bar. However, it increased to between 0.100-0.125 bar after just some weeks, reducing the available driving force. Based on the new flow rate the hydraulic resistance of the bed should produce a lower pressure drop of 18 mbar/m at 10°C or 0.04 bar in total. Considering the static zero offset (no flow) of ca 0.05 bar, the initial pressure drop should be around 0.09 bar without any fouling. This is in line with the values directly after bed lowering, however the subsequent increase in initial pressure drop suggests a progressing fouling of the bed.

Evolution of Hydraulic Resistance Across Bed Layers

The mini-column test was also done twice after lowering of the bed to first see if it had changed and then to track its change over time. The pressure profiles can be seen in Figure 4.13 with the first test for comparison. For raw data see Table A1, A3 and A4.

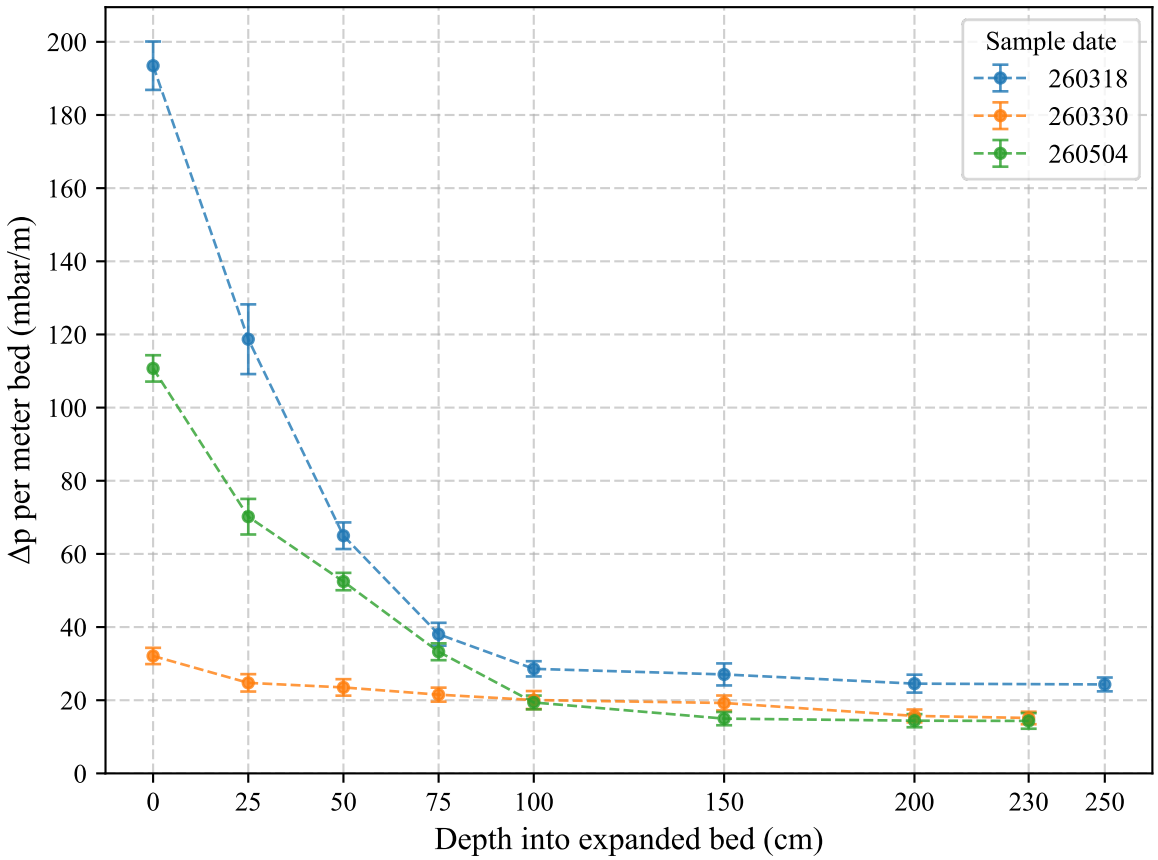

Figure 4.13. Pressure profile as the pressure loss per meter bed (mbar/m) for GAC collected at different expanded bed depth before bed lowering (blue) and shortly after (orange) as well as after about a month after bed lowering (green).

Following bed lowering a significant decrease in the hydraulic resistance in the top layers could be confirmed with GAC retrieved 2026-03-30. The decrease in pressure drop per meter for the top layers in the pressure profile were reflected in the operational results with respect to filter run time and TSS load per run as was seen previously. Thus, the bed lowering was successful in remediating the hydraulic resistance of the top layers. The decrease is reasonable as the bed lowering targeted the top layers of the bed following the localisation based the first test. At this point most of particles with a distinct brownish colour had been removed and the top GAC was more akin to new GAC in colour. Unlike before bed lowering, the resistance for some depths were lower than that of new GAC. Because PSD tests confirmed (see Evolution of Particle Size Distributions), the particle size had shifted to generally larger particles, the baseline resistance for each depth could be reduced.

After a month following the second mini-column test, GAC retrieved 2026-05-04 shows a resurgence in the hydraulic resistance of the top 50 cm of the expanded bed. From 100 cm onwards the hydraulic resistance matches that of the previous attempt and is still lower than before bed lowering. This indicates that the changes to the bed that is causing the resistance is

primarily happening at the top and is approaching the conditions prior to bed lowering. This increase is progressing despite an attempted more aggressive backwashing (see Backwashing).

Evolution of Particle Size Distributions

Two additional PSD tests were conducted after the lowering of the bed, to track changes over time and for comparison before the change. The results are plotted with the results from before the bed was lowered in Figure 4.14 along with the result for new GAC. For the raw data, see Appendix B1, B2, B4, B5.

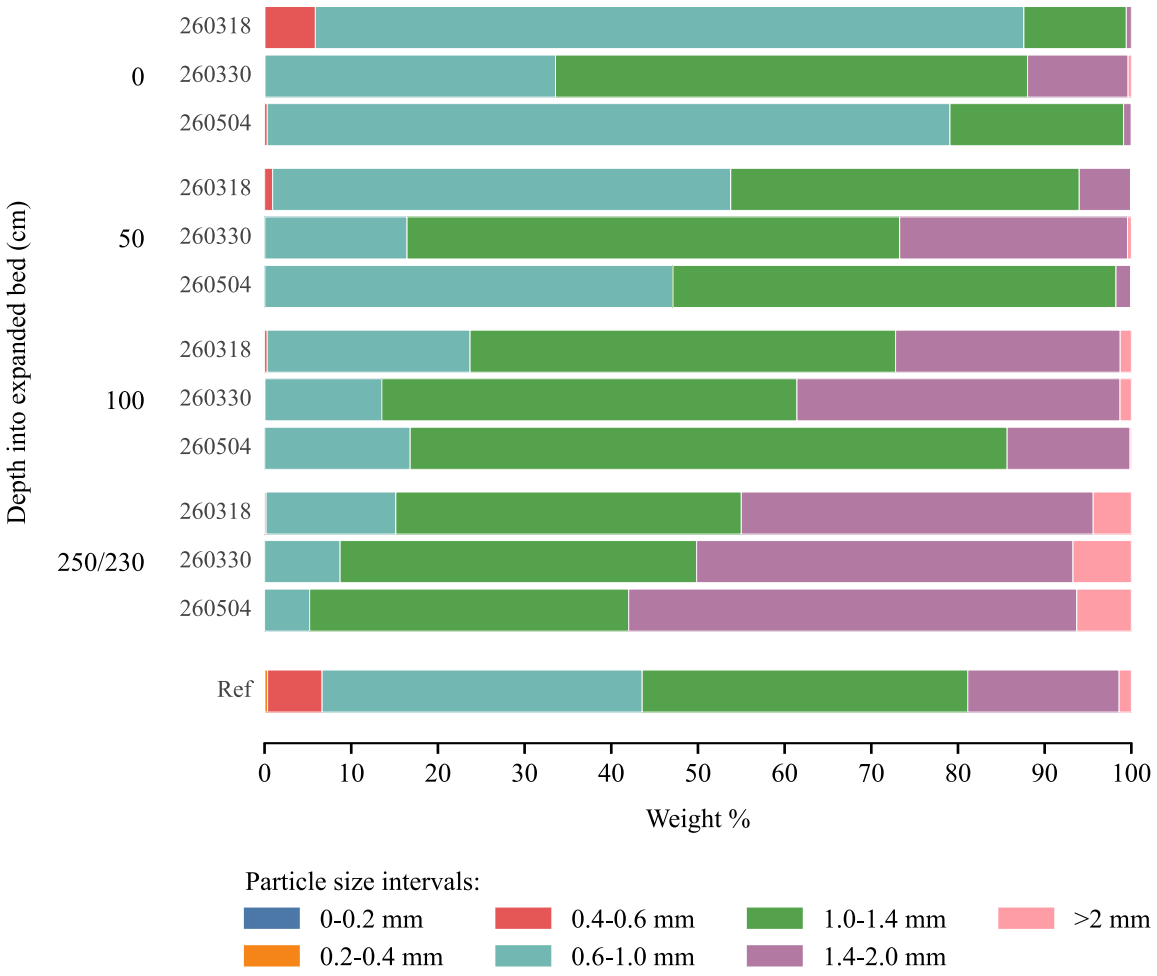

Figure 4.14. Particle size distributions (PSDs) for GAC collected at different depths into the expanded bed before bed lowering, shortly after and after about a month after bed lowering.

In general, it appears larger particles sizes are more prominent at all depths following the bed lowering for GAC retrieved both 2026-03-30 and 2026-05-04. This could be because of wash-out of primarily small particles during bed lowering. Immediately following bed lowering particles in larger particle size intervals are seen at greater amounts further up in the bed. For instance, the particle size interval 1.4-2.0 mm is considerably more prominent in the second

PSD with even some particles above 2.0 mm being present. The smallest particle size interval before lowering of the bed, 0.4-0.6 mm, is absent for all depths immediately after lowering the bed. Altogether, the generally larger particles at all depths could partly explain the more uniform appearance in the pressure profile test and the more slowly increasing pressure drop curves.

In the final test following bed lowering, larger particle size intervals are more predominant deeper into the bed. Conversely, smaller particles are more predominant further up the bed. This indicates that the bed has either become more stratified, similarly to before the bed was lowered, but with the distributions skewed more to larger particles sizes across all depths. The 0.4-0.6 mm particle size interval has reappeared for the top layer, but not to a great extent (less than 1%). This could be a result of abrasion following the increase in air scouring in the backwashing program (see Backwashing). Altogether, there is stratification of the bed in all tests, but by varying degrees. This is indicative of a well-functioning backwashing program. However, stratification could help explain the tendency of the pressure drop curve to shift from a slowly to a more rapidly increasing appearance, which indicates a surface filtering effect (Schölzer et al., 2022). Stratification according to material density and particle size after just a few backwashes has also been confirmed elsewhere (Frank et al., 2015). This could explain the difference in distributions between the second and third PSD after just a month. Apart from the surface filtration effect, stratification has also been shown to enhance adsorptive capabilities at the top of the GAC bed and diminish them at the bottom with respect to MP removal, DOC removal, and UVA_{254} removal (Frank et al., 2015).

Backwashing

Following bed lowering, more aggressive backwashing programs could be used due to the increased headroom between bed and overflow channel. To assess the performance of the backwashing programs, mass balances were made for several runs following the change in bed height for filter runs on April 7 (24.3h), April 8 (22.9h), April 12 (17.9h), April 15 (6.8h, not complete), April 28 (12.4h) and April 29 (11.3h), see Appendix C for more information. For the raw TSS data, see Table C5-C10. The first program used from March 24 to April 7, 2026, can be seen in Table C1. It uses an initial 60 s air scouring, two ensuing water phases to carefully remove bubbles while preventing GAC washout and a final water phase producing 40% expansion (45 cm below the overflow) to wash away TSS. In Table 4.1 the results from backwashing can be seen.

Table 4.1. For different filter cycles, the TSS load and total TSS retained by the filter, the TSS concentration in the backwash water phases and the total TSS backflushed. The difference is between the TSS retained by the filter and the total TSS backflushed. A negative value indicates more TSS was removed during backwashing than what was retained during the filter run.

Filter run	TSS load (g)	TSS retained by filter (g)	TSS backwash water (mg/L)	Total TSS backflushed (g)	Difference (g)
260407	478	278	W1: 67 ± 12 W2: 32 ± 3	289	-11
260408	430	308	W1: 200 ± 23 W2: 56 ± 2	489	-181
260412	410	293	W2: 78 ± 3	577	-284
260415	303	193	W2: 56 ± 4	422	-229
260428	292	216	W2: 47 ± 5	358	-142
260429	340	252	W2: 51 ± 6	381	-129

Table 4.1 indicates that all the TSS retained by the filter was washed away using the first program. Between April 8-12, the second phase was replaced by a second air scouring phase at 60 s to see if it had an impact on the removed TSS. Both air scouring phases were also increased in intensity. The results suggest that for about the same TSS load and TSS retained by the filter, more TSS is removed during backwashing following the increase in air scouring. The results also suggest that more TSS is removed than is retained by the filter. In Figure 4.15 the initial pressure drop for filters runs for the entire remediation period can be seen.

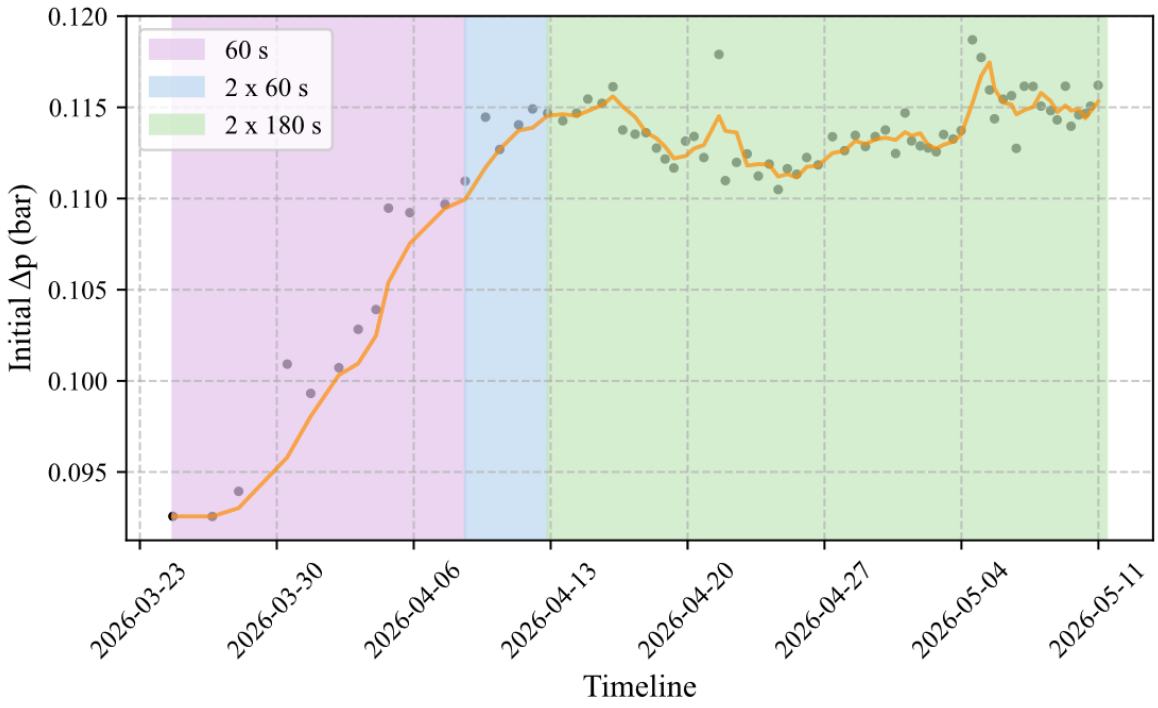

Figure 4.15. The initial pressure with the periods of different air scouring duration. The orange line is the 3-cycle moving average in initial pressure.

To curb the increase in initial pressure in Figure 4.15, the duration of the air scouring phases was further increased to 180 s, see complete program in Table C2. This was done as subsequent air sequences of 2-3 min have been recommended from literature to combat biofilm growth (Schölzel et al., 2022). The intensity was not further increased to limit abrasion of GAC. The air scouring flow rate could not be measured, but the dispersion of air appeared even and reminiscent of a rolling boil. The repeated results that more TSS was removed during backwashing than what was retained in the filter indicates the programs with increased air scouring were successful in removing the TSS retained by the filter and even the entire TSS load per run. The extra TSS removed could be previously accumulated TSS, growth from the sides of the GAC filter or biofilm on the particles. From Figure 4.15 the more aggressive air scouring also suggests the rise in initial pressure was curbed. Because backwashing primarily removes the outer layers of biofilm, and not the entrenched biofilm in the macropores (Fundneider et al., 2021b), it is reasonable that more aggressive backwashing would decrease the initial hydraulic resistance.

Potential in Optimising Water Usage

For the filter cycle on April 28, 2026, about 11% of the treated water was used for backwashing. To investigate if the water usage could be shortened a TSS concentration profile was made based on the water phase to understand how it behaves during backwashing (blue line), see Figure 4.16 and Table C11 for raw data.

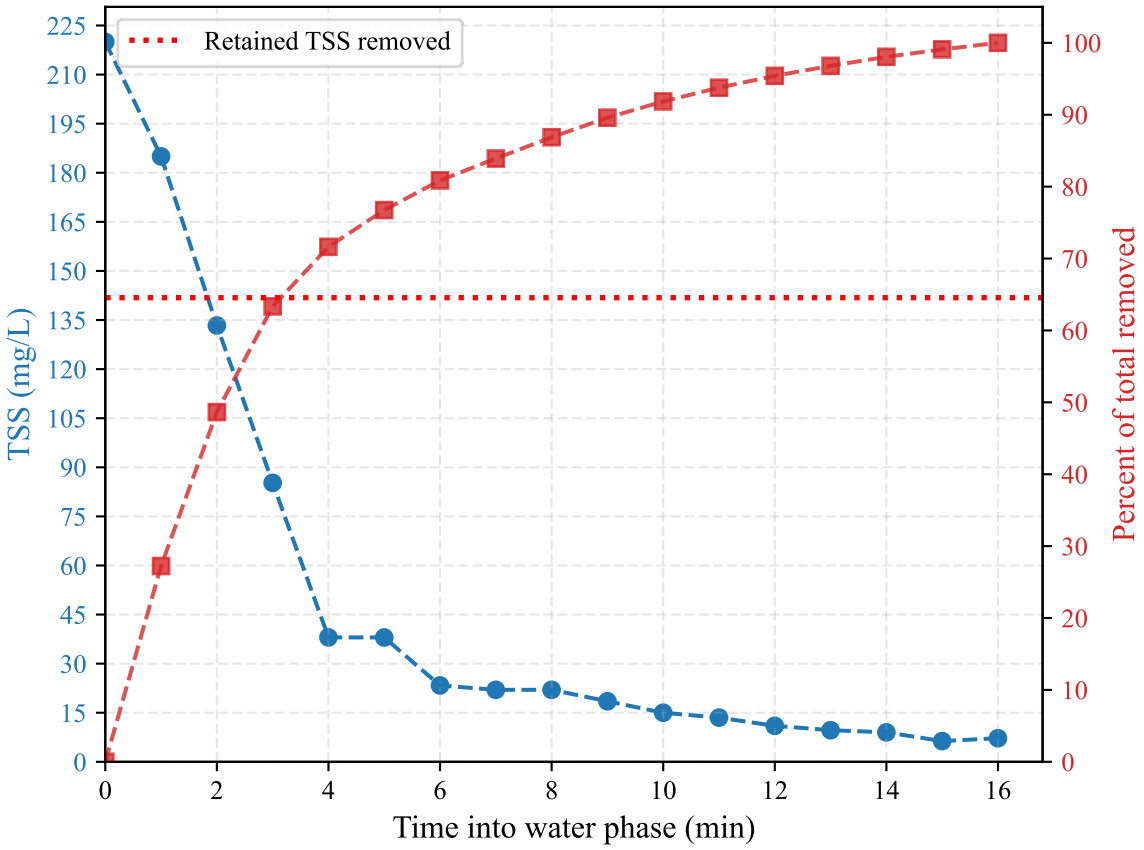

Figure 4.16. The change in concentration of TSS in the backwashing water can be seen in blue. In red, the percent removed at that time into the water phase. The red line marks the point at which the TSS retained during the filter run has been removed.

From a high of 220 mg/L, it quickly decreases during the first 5 minutes to 38 mg/L and down to about 6-7 mg/L by the very end, which is in the same order of magnitude as the influent TSS concentration. Based on the total mass removed during backwashing, the percent removed at that time into the water phase can be plotted along with the retained TSS in percent of the total removed to find diminishing returns. At 4 minutes, the estimated retained TSS mass from the filter run had been removed. Thus, there is a possibility for optimisation in water usage to limit the hypothetical future increase in hydraulic load at Rya WWTP. However, this must be further evaluated for certainty, which could not be done due to time constraints.

4.2 Treatment Results & Discussion

The removal of standard parameters will be reviewed, followed by treatment performance of the directive substances and PFAS-24.

4.2.1 Removal of Standard Parameters

Figure 4.17 and figure 4.18 shows how the treatment of the the standard parameter varies with the BVs treated. In Table 4.2 the mean influent and standard deviations and number of samples can also be seen.

Table 4.2. The mean influent values for the standard paramters and the number of samples tested.

Parameter	Influent GAC	Number of samples
TSS (mg/L)	4.1 ± 2.1	30
UVA_{254} (m^{-1})	22.2 ±1.9	30
DOC (mg C/L)	10.9 ± 1.5	25
TOC (mg C/L)	15.2 ± 6	6
COD (mg O_2/L)	44 ± 5.3	6
BOD (mg O_2/L)	6.9 ± 1.7	6
P_{tot} (mg/L)	0.27 ± 0.07	6
PO_4-P (mg/L)	0.09 ± 0.03	6
N_{tot} (mg/L)	6.3 ± 3.0	6
NH_4-N (mg/L)	3.7 ± 3.0	6
NO_3-N (mg/L)	1.1± 0.5	6
NO_2-N (mg/L)	0.16 ± 0.06	6

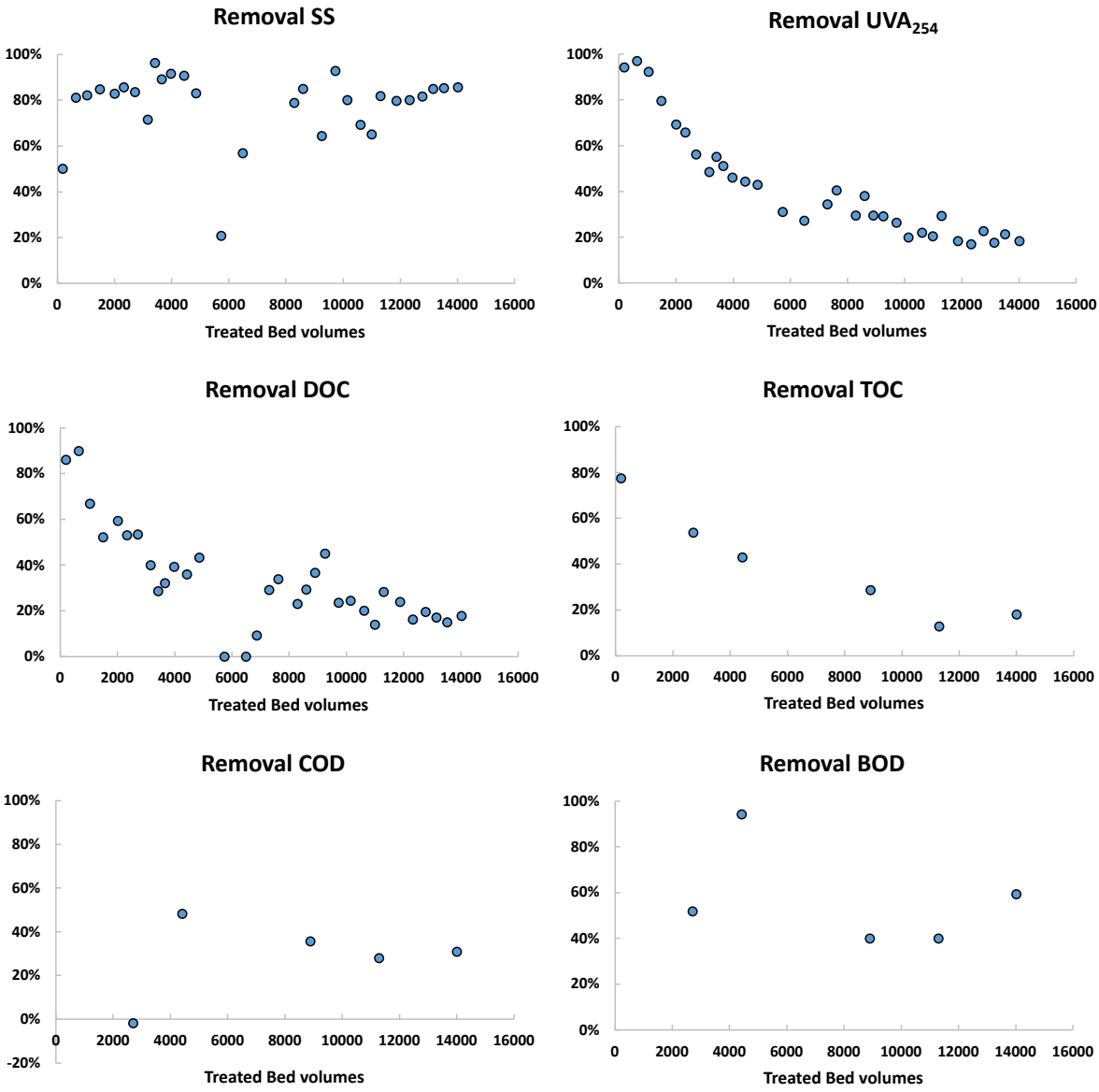

Figure 4.17. Treatment results for several standard parameters with the BVs treated.

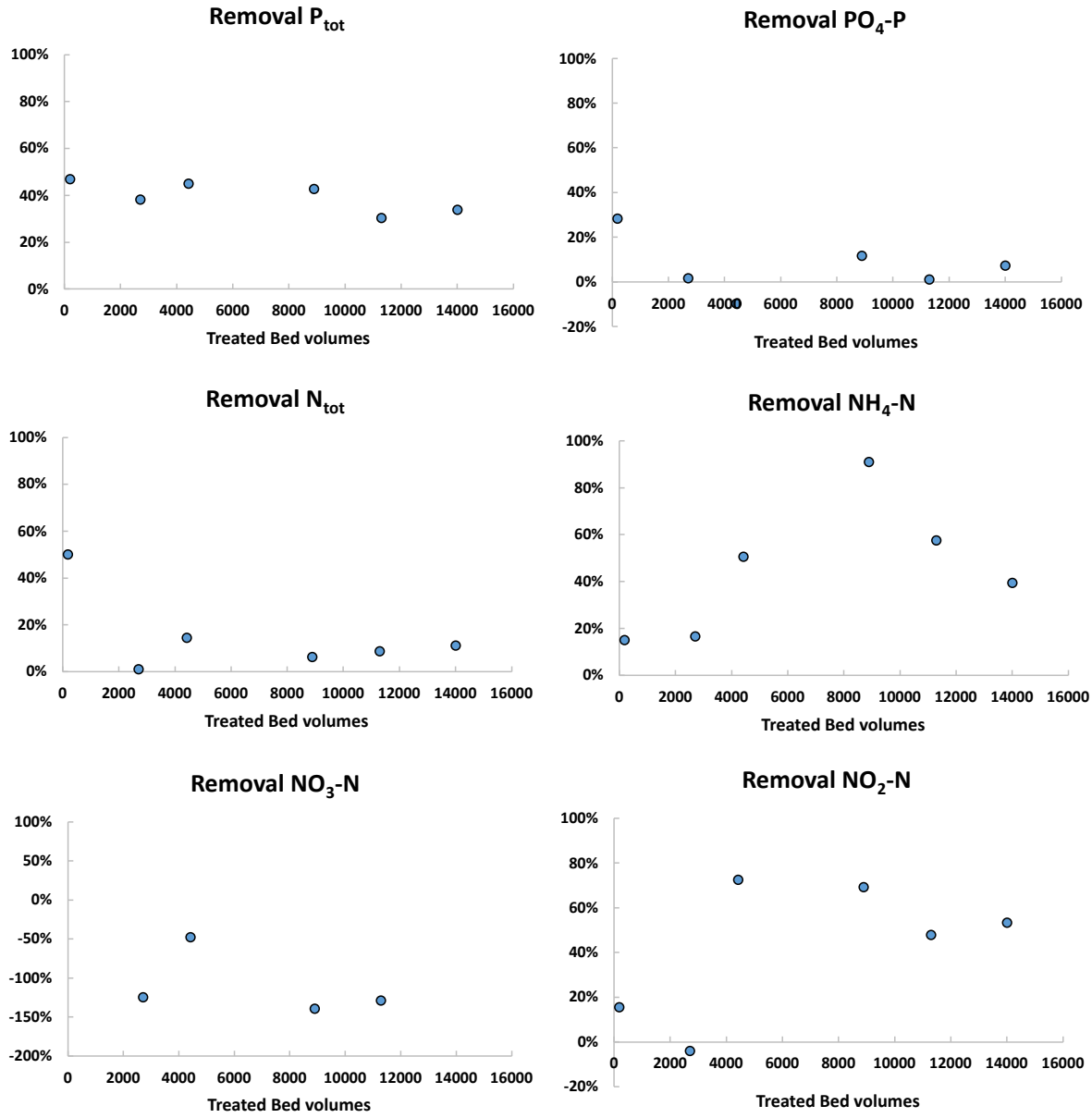

Figure 4.18. Treatment results for additioal standard parameters with the BVs treated.

TSS decreases quite singificantly in the filter at (~80%), which has been confirmed previously (Juarez et al., 2026). Both DOC and UVA_{254} exhibit high inital removal, which is usually attributed to adsorption. It typically stabilises to around 0-20% removal, which is usually attributed to residual biodegradation by biofilm. Overall, this behaviour has been previously confirmed (Juarez et al., 2026). Moreover, TOC and COD largely follow the same trend as DOC, which has also been previously confirmed (Juarez et al., 2026). Regarding BOD, it is reduced by ~40% or more in the GAC filter, this could be due to particulate BOD being retained or due to uptake by biofilm in the filter. The elimination of BOD has also been confirmed elsewhere (Juarez et al., 2026), but the effluent concentrations are often not reported rendering exact comparisons of the degree of removal difficult to make. Moreover, P_{tot} was reduced in the filter, and because PO_4-P is relatively unchanged, it can likely be attributed to the removal

of TSS and has been previousy observed (Juarez et al., 2026). The removal in N_{tot} is negligible, but based on the removal in NH_4-N, along with the increase in NO_3-N, it appears there is some nitrification in the filter. This can be related to the preceding nitrifying MBBR, resulting in colonisation by nitrifiers entrained in the water (Juarez et al., 2026). A prerequesitve for nitrification is a sufficient DO-level, which has been obsererved in this GAC pilot.

4.2.2 Removal of Micropollutants

The most favourable combination of substances according to the UWWTD and the removal across all the substances can be seen in Figure 4.19 plotted with increasing BVs treated.

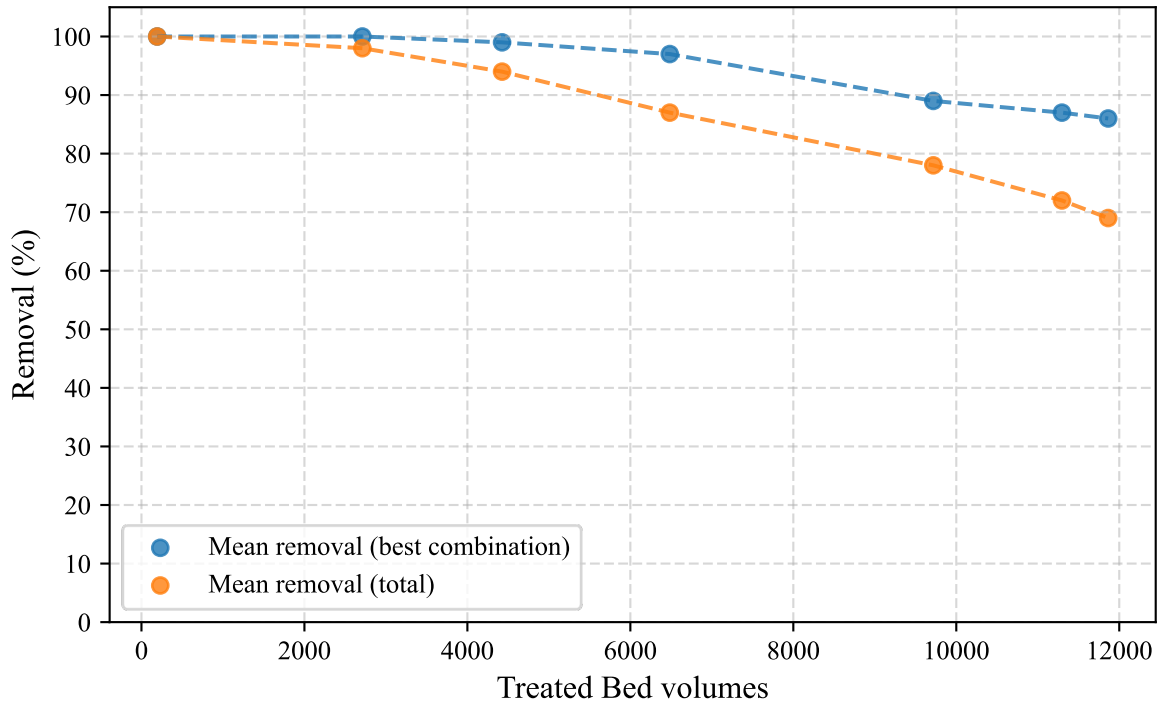

Figure 4.19. How the mean removal of all 12 and the best combination of indicator substances selected in accordance with the UWWTD changes with the number of BVs treated.

If the best combination of substances in accordance with the directive are chosen, the GAC pilot achieves a mean of 86% removal after almost 12,000 BV. However, this constitutes insufficient operational time to evaluate the final operating costs, but reaching at least 20,000 BV would be desirable. For the same BVs treated, the mean total removal across all key indicators was 69%. Another pilot project with a GAC filter at a similar EBCT of 21.8 min, a bed height of 1.5 m consisting of GAC with a particle size of 1.2-2.3 mm achieved a mean of 82-88% for all 12 indicator substances after ca 12,000 BV at an influent DOC concentration of almost 6 mg/L (Böhler et al., 2020). This is comparatively better treatment performance than this GAC pilot. The difference could be explained by the almost twice as high mean DOC concentration of 10.9 mg/L for the GAC pilot at Rya WWTP, which can compete with the MPs for adsorption sites (Böhler et al., 2020). At the same time, the grain size of this GAC pilot is smaller, which should have a positive effect on performance.

It should be noted that there are also uncertainties associated with these figures due to the long periods of frequent backwashing and operational downtimes. However, it stills serves as an indication that the GAC filter can treat the directive substances based on the water matrix. In addition, these numbers reflect only the removal by the GAC pilot, whereas the total removal mandated by the UWWTD is based on the removal over the whole WWTP.

Figure 4.20 shows how the elimination of all directive substances changes with the number of BVs treated.

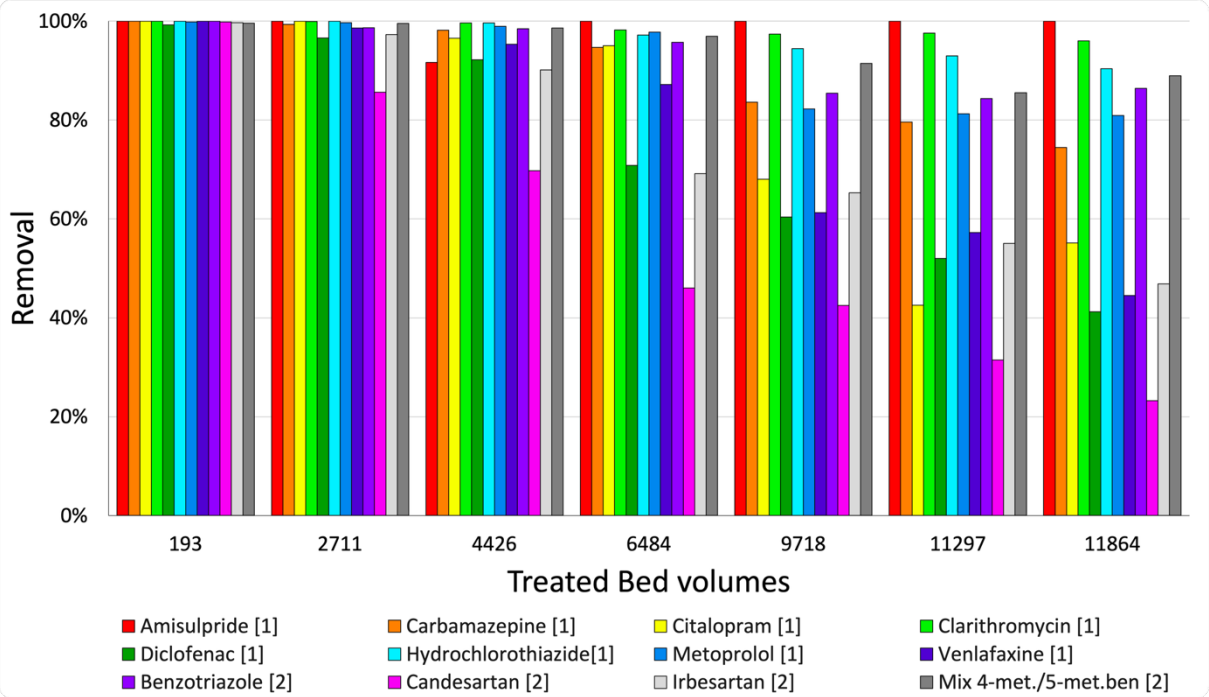

Figure 4.19. How the removal of all 12 directive substances (marked by category) changes with the number of BVs treated.

Initially the treatment is high for all the directive substances, but after ~4,500 BV they exhibit varying removal. The removal of citalopram (55%), diclofenac (41%), venlafaxine (44%), candesartan (23%) and irbesartan (47%) have decreased most significantly at ~12,000 BVs treated. Conversely, amisulpride (100%), carbamazepine (74%), hydrochlorothiazide (90%), metoprolol (81%), clarithromycin (96%), benzotriazole (86%) and the mixture (89%) exhibit better performance. A comparison to the GAC pilot from Böhler et al. (2020) after ~12,000 BVs treated can be seen in Table 4.3.

Table 4.3. Comparison of the treatment performance of individual MPs from the UWWTD between the Rya GAC pilot and Böhler et al. (2020) after ~12,000 BVs treated.

Indicator Substance	Rya GAC pilot (%)	Böhler et al. (2020) (%)
Amisulpride	100	~100
Carbamazepine	74	~80-92
Citalopram	55	~100
Clarithromycin	96	~80-85
Diclofenac	41	~77-89
Hydrochlorothiazide	90	~88-95
Metoprolol	81	~90-94
Venlafaxine	44	~88-93
Benzotriazole	86	~90-93
Candesartan	23	~39-52
Irbesartan	47	~62-78
Mixture of 4-methylbenzotriazole and 5-methylbenzotriazole	89	~90-93

From Table 4.3, the GAC pilot at Rya WWTP performs similarly or worse for all MPs except clarithromycin. Amisulpride, carbamazepine, hydrochlorothiazide, metoprolol, benzotriazole and the mixture all perform comparably and maintain good elimination at ~12,000 BV. However, citalopram performs considerably worse in the GAC pilot at Rya WWTP, as does diclofenac and venlafaxine. Candesartan is the worst performer out of all directive substances and exhibits a rapid decrease in performance for both GAC filters. Irbesartan also shows poor elimination in both GAC filters, but worse in the GAC pilot at Rya WWTP.

A subset of largescale and pilot-scale downflow GAC filters from a meta-analysis by Benstoem et al. (2017) with DOC in the range of 5.5–11.4 mg/L and EBCT between 19–25 min exhibit an 80% removal breakthrough at 4,700 to 20,000 BVs for carbamazepine, and 4,100 to 20,000 BV for diclofenac. For the GAC pilot at Rya WWTP, 80% removal occurs after 4400-6500 BV for diclofenac, which is in the lower range, but at 11,200 BV for carbamazepine, which is intermediate.

PFAS-24 Treatment

Figure 4.21 shows how the removal of PFAS-24 treatment changes with the BVs treated.

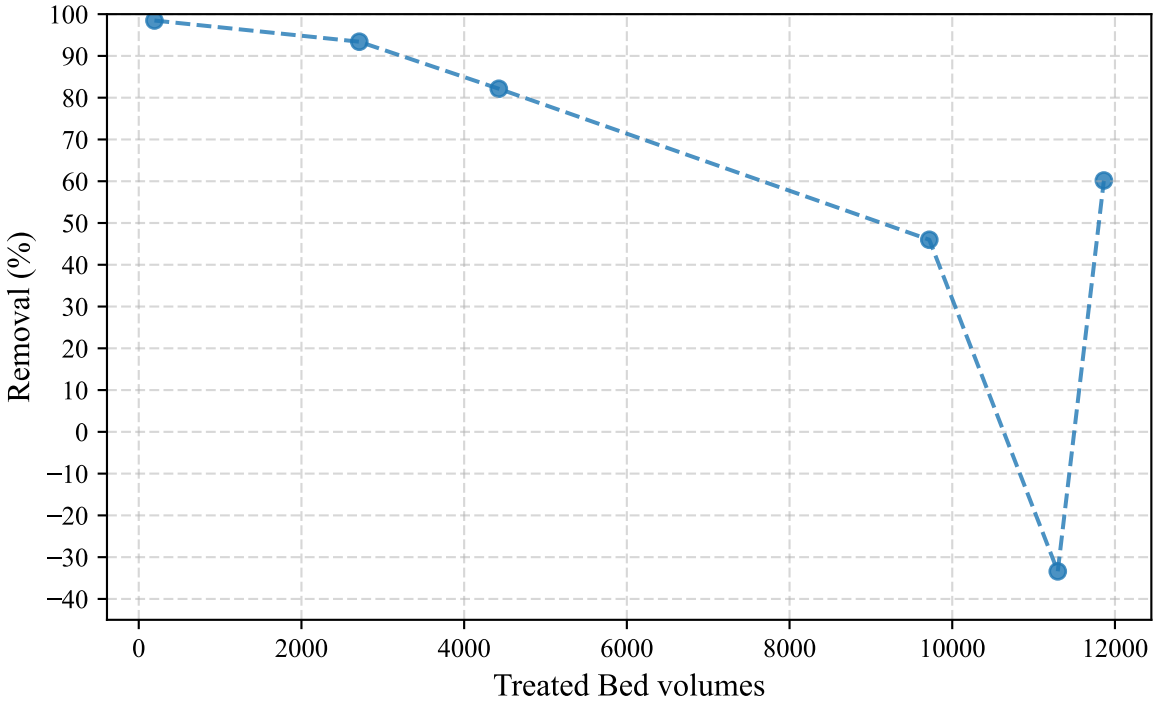

Figure 4.21. How the removal of PFAS-24 changes with the number of bed volumes treated.

The removal of PFAS-24 can be confirmed in the GAC pilot, with almost complete removal initially, but it then tapers down faster than for the directive substances. By ~5,000 treated BVs, the removal of PFAS-24 is most likely already below 80% and at ~10,000 treated BVs, it is below 50%. If treatment requirements for PFAS are introduced, the bed may need to be replaced often, leading to high operational costs. Interestingly, the figure indicates that PFAS were desorbed as there is negative elimination just before the bed was lowered (11300 BVs). It should be noted that a similar decrease in the removal of MPs at the same treated BVs was not observed, which means this could be a measurement error. Following the lowering of the bed it appears PFAS removal is again observed. More data points are required to say anything definitively.

Removal of PFAS have been previously confirmed for GAC filters in drinking water treatment with decreasing removal for most PFAS species with increasing number of BVs treated (Appleman 2014; McCleaf et al., 2017). Differences in treatment efficiency and BVs treated until breakthrough has been partly attributed to chain length, where higher removal efficiency has been maintained for longer with increasing chain length while short-chain PFAS have even been seen to desorb (Appleman et al., 2014; McCleaf et al., 2017). In addition, PFAS containing sulfonic acids have exhibited better removal and slower breakthrough than those with carboxylic acids as functional groups (Appleman et al., 2014, McCleaf et al., 2017). Moreover, linear isomers have been observed to maintain higher removal than branched isomers with increasing BVs treated (McCleaf et al., 2017).

5 Conclusions

The following can be concluded regarding the hydraulic and treatment performance of GAC pilot:

- The hydraulic performance of the GAC pilot has decreased over time with respect to filter run times and TSS load per run from 12.3 ± 5.9 h and 270 ± 118 g TSS between July to October 2025, down to 3.0 ± 2.2 h and 96 ± 92 g TSS between October 2025 to March 2026, with as low as 1.5 ± 0.4 h and 37 ± 13 g TSS for the worst sustained period.
- No strong correlation was found between decreasing filter run times and mean influent TSS concentration pointing to other factors such as biofilm growth are affecting the hydraulic performance negatively.
- The initial pressure for the filter runs increases over time, reducing the available driving force per run, which can contribute to shorter filter runs.
- Biofilm growth was confirmed on the particles with microscopy, in the GAC pilot and in the influent and effluent tanks, which can be a primary reason for poor hydraulic performance. The occurrence of biofilm growth in the GAC pilot is further supported by high DO consumption, BOD removal and decreasing NH_4-N and increasing NO_3-N concentrations, which suggest nitrification is occurring in the bed.
- A method was developed that enabled localisation of the hydraulic resistance to the top of the filter. Removal of the top layers of GAC temporarily improved the filter run time and increased the TSS load per run. Despite more aggressive backwashing programs which indicated more TSS is washed out than is retained, the hydraulic resistance in the top layers returned and had a negative impact on filter run time and attainable TSS load per run.
- Most of the TSS retained during filter runs were removed during the first minutes of the water phase, suggesting that the backwashing programs can be further optimised.
- The bed becomes stratified by backwashing which is likely contributing to a surface filtration effect that could be further exacerbated by biofilm growth in shortening the filter run time and attainable TSS load.
- TSS, P_{tot} and BOD were all significantly removed, whereas N_{tot} and PO_4-P removal were negligible throughout the operational history of the GAC pilot. Both UVA_{254} and DOC have tapered to ~20% of their influent concentrations at ~14,000 treated BV.
- The GAC pilot can successfully remove 6 indicator substances in a 2:1 ratio with 86% removal in accordance with the UWWTD after ~12000 BVs treated. For all 12 indicators combined, the mean removal is 69%. Frequent backwashing and operational downtime could have impacted the results.
- The removal of PFAS-24 decreases faster than for the MPs to below 80% after ~5,000 BVs treated which indicates frequent exchange of GAC is required to maintain high treatment targets.

6 Future Studies

Suggested further research include:

- Investigate and characterise the biofilm growth. For instance, oxygen depletion and quantification of the extent of growth at different depths in the bed and identification of the types of microorganisms on the granules.
- Characterisation of the incoming TSS to investigate if their properties could have an impact on the reduced hydraulic performance.
- Optimisation of the backwashing programs to limit water use.
- Consider fluidised GAC filters without particle retention or upflow filters which feature coarse-to-fine PSD in the flow direction.

7 References

Appleman, T.D., Higgins, C.P., Quiñones, O., Vanderford, B.J., Kolstad, C., Zeigler-Holady, J.C. and Dickenson, E.R.V. (2014). Treatment of poly- and perfluoroalkyl substances in U.S. full-scale water treatment systems. *Water Research*, 51, pp. 246–255. Available at: https://doi.org/10.1016/j.watres.2013.10.067.

Benstoem, F., Nahrstedt, A., Boehler, M., Knopp, G., Montag, D., Siegrist, H., & Pinnekamp, J. (2017). Performance of granular activated carbon to remove micropollutants from municipal wastewater - A meta-analysis of pilot- and large-scale studies. *Chemosphere*, 185, 105-118. Available at: https://doi.org/10.1016/j.chemosphere.2017.06.118

Betsholtz, A. (2023) *Adsorption and transformation of organic micropollutants in wastewater: New insights from 14C-labeling*. Doctoral thesis. Lund University.

Bourgin, M., Beck, B., Boehler, M., Borowska, E., Fleiner, J., Salhi, E., Teichler, R., von Gunten, U., Siegrist, H. and McArdell, C. S. (2018). Evaluation of a full-scale wastewater treatment plant upgraded with ozonation and biological post-treatments: Efficacy in micropollutant removal, toxicity reduction and ozone oxidation by-product formation. *Water Research*, 133, pp. 238-253. Available at: https://doi.org/10.1016/j.watres.2017.10.036

Busck, M., Takman, M., Blomqvist, S., Svahn, O., Davidsson, Å. and Cimbritz, M. (2026). Full-scale quaternary treatment of municipal wastewater using granular activated carbon: long-term removal of organic micropollutants. *Water Practice and Technology*, 21(1), pp. 266–274. Available at: https://doi.org/10.2166/wpt.2025.181

Böhler M., Joss A., McArdell C., Brander A. (2023). Faktenblatt – aktueller Stand diskontinuierlich gespülte GAK-Filterzur Elimination organischer Spurenstoffe aus kommunalem Abwasser. Konsenspapier zum Ergebnis eines Workshops mit Fachexperten aus der Schweiz und Deutschland, Eawag und VSA, Dübendorf. Aktualisierte Version 2 des Konsenspapiers von 2020.

Böhler, M., Hernandez, A., Baggenstos, M., McArdell, C.S., Siegrist, H., Joss, A. (2020). Elimination von Spurenstoffen durch granulierte Aktivkohle-Filtration (GAK): Grosstechnische Untersuchungen auf der ARA Furt, Bülach, Schlussbericht Eawag, Dübendorf, Schweiz.

Çeçen, F. and Aktaş, Ö. (2011). *Activated Carbon for Water and Wastewater Treatment: Integration of Adsorption and Biological Treatment*. 1st ed. Weinheim: WILEY-VCH Verlag GmbH & Co. KGaA.

Chemviron 2020a. Cyclecarb 401 - High performance Reactivated Carbon Data Sheet. Chemviron.

Chemviron 2020b. Installation commissioning and backwashing - Filtrasorb® GAC adsorbers for water treatment. Chemviron.

Cleasby, J.L. and Baumann, E.R. (1974). Wastewater filtration design considerations. U.S. Environmental Protection Agency Technology Transfer.
Crittenden, J.C., Trussell, R.R., Hand, D.W., Howe, K.J. and Tchobanoglous, G. (2012). Granular Filtration. In MWH's Water Treatment: Principles and Design, Third Edition (eds J.C. Crittenden, R.R. Trussell, D.W. Hand, K.J. Howe and G. Tchobanoglous).

European Parliament and Council of the European Union (2024). Directive (EU) 2024/3019 of the European Parliament and of the Council of 27 November 2024 concerning urban wastewater treatment. *Official Journal of the European Union*, L 3019. Available at: https://eur-lex.europa.eu/legal-content/EN/TXT/?uri=CELEX%3A02024L3019-20241212 (Accessed: 26 May 2026)

European Parliament and Council of the European Union (2013). Directive 2013/39/EU of the European Parliament and of the Council of 12 August 2013 amending Directives 2000/60/EC and 2008/105/EC as regards priority substances in the field of water policy. *Official Journal of the European Union*, L 226, pp. 1-17. Available at: https://eur-lex.europa.eu/legal-content/EN/TXT/?uri=CELEX:32013L0039 (Accessed: 26 May 2026)

Frank, J., Ruhl, A.S. and Jekel, M. (2015). Impacts of backwashing on granular activated carbon filters for advanced wastewater treatment. *Water Research*, 87, pp. 166-174. Available at: https://doi.org/10.1016/j.watres.2015.09.020.

Fundneider, T., Acevedo Alonso, V., Abbt-Braun, G., Wick, A., Albrecht, D. and Lackner, S. (2021a). Empty bed contact time: The key for micropollutant removal in activated carbon filters. *Water Research*, 191, p. 116765. Available at: https://doi.org/10.1016/j.watres.2020.116765.

Fundneider, T., Acevedo Alonso, V., Wick, A., Albrecht, D. and Lackner, S. (2021b). Implications of biological activated carbon filters for micropollutant removal in wastewater treatment. *Water Research*, 189, p. 116588. Available at: https://doi.org/10.1016/j.watres.2020.116588.

Ianes, E., Lolić, A., Ukić, Š., Kučić Grgić, D., Bolanča, T. and Cvetnić, M. (2025). Micropollutants removal, residual risk, and costs for quaternary treatments in the framework of the Urban Wastewater Treatment Directive. *Water Research X*, 29, p. 100334. Available at: https://doi.org/10.1016/j.wroa.2025.100334

Juárez Cámara R., Andén T., Edefell E., Bengtsson S., Wetterborg Karlsson C., Widell B., Tumlin S., Betsholtz A., Björksund-Tuominen M. och Mattsson A. (2025). Samverkan mellan konventionell och kvartär avloppsrening. En kunskapssammanställning. SVU-rapport 2026-2. Stockholm: Svenskt Vatten.

Lofrano, G., Brown, J. (2010). Wastewater management through the ages: A history of mankind. *Science of The Total Environment, Volume 408, Issue 22*, 5254–5264. Available at: https://doi.org/10.1016/j.scitotenv.2010.07.062

McCleaf, P., Englund, S., Östlund, A., Lindegren, K., Wiberg, K. and Ahrens, L. (2017). Removal efficiency of multiple poly- and perfluoroalkyl substances (PFASs) in drinking water using granular activated carbon (GAC) and anion exchange (AE) column tests. *Water Research*, 120, pp. 77–87. Available at: https://doi.org/10.1016/j.watres.2017.04.057.

Naturvårdsverket (2026). Förslag till författningsändringar till följd av EU:s reviderade avloppsvattendirektiv. Available at: https://www.naturvardsverket.se/490731/contentassets/5408c5e2928d421fafbafa70a30651e4/forslag-till-forfattningsandringar-till-foljd-av-eus-reviderade-avloppsvattendirektiv.pdf (Accessed: 26 Maj 2026)

Pistocchi, A., Andersen, H.R., Bertanza, G., Brander, A., Choubert, J.M., Cimbritz, M., Drewes, J.E., Koehler, C., Krampe, J., Launay, M., Nielsen, P.H., Obermaier, N., Stanev, S., Thornberg, D. (2022). Treatment of micropollutants in wastewater: Balancing effectiveness, costs and implications. *Science of The Total Environment*, 850, p. 157593. Available at: https://doi.org/10.1016/j.scitotenv.2022.157593

Ripperger, S., Gösele, W., & Alt, C. (2012). Filtration, 1. Fundamentals. In *Ullmann's Encyclopedia of Industrial Chemistry* (Vol. 14, pp. 678–709). Wiley-VCH Verlag GmbH & Co. KGaA, Weinheim.

Rizzo, L., Malato, S., Antakyali, D., Beretsou, V. G., Đolić, M. B., Gernjak, W., Heath, E., Ivancev-Tumbas, I., Karaolia, P., Lado Ribeiro, A. R., Mascolo, G., McArdell, C. S., Schaar, H., Silva, A. M. T. and Fatta-Kassinos, D. (2019). Consolidated vs new advanced treatment methods for the removal of contaminants of emerging concern in urban wastewater. *Science of The Total Environment*, 655, pp. 986-1008. Available at: https://doi.org/10.1016/j.scitotenv.2018.11.265

Sbardella, L., Comas, J., Fenu, A., Rodriguez-Roda, I. and Weemaes, M. (2018). Advanced biological activated carbon filter for removing pharmaceutically active compounds from treated wastewater. *Science of The Total Environment*, 636, pp. 519-529. Available at: https://doi.org/10.1016/j.scitotenv.2018.04.214

Schölzel et al. (2022). Dimensionierung großtechnischer GAK-Filter durch Ermittlung der erzielbaren Feststoffbelastungen und Spülintervalle (SOLIDUS). Kurzbericht zum gleichnamigen Forschungsvorhaben, gefördert vom Ministerium für Umwelt, Landwirtschaft, Natur- und Verbraucherschutz des Landes Nordrhein-Westfalen.

Svahn, O., & Björklund, E. (2016). Increased electrospray ionization intensities and expanded chromatographics possibilities for emerging contaminants using mobile phases of different pH. *Journal of Chromatography B, 1033, 128-137.* Available at: 10.1016/j.jchromb.2016.07.015

Svahn, O., & Björklund, E. (2019). High Flow-Rate Sample Loading in Large Volume Whole Water Organic Trace Analysis Using Positive Pressure and Finely Ground Sand as a SPE-Column In-Line Filter. *Molecules, 24(7), 1426.* Available at: https://doi.org/10.3390/molecules24071426

Svahn, O., & Björklund, E. (2024). Assessment of full-scale 4th treatment step for micro pollutant removal in Sweden: Sand and GAC filter combo. *Science of The Total Environment, Volume 906*, 2024, 167424, ISSN 0048-9697, Available at: https://doi.org/10.1016/j.scitotenv.2023.167424.

Takman, M., Betsholtz, A., Davidsson, Å., Cimbritz, M., Svahn, O., Karlsson, S., Østergaard, S.K., Nielsen, J.L. and Falås, P. (2024). Biological degradation of organic micropollutants in GAC filters–temporal development and spatial variations. *Journal of Hazardous Materials*, 472, p. 134449. Available at: https://doi.org/10.1016/j.jhazmat.2024.134449.

Tchobanoglous, G., Burton, F.L. and Stensel, H.D. (2003). *Wastewater engineering: treatment and reuse*. 4th ed. Boston: McGraw-Hill.

Videbris, K.-E. (2025). Miljörapport Gryaab, Ryaverket 2024. Göteborg: Gryaab AB. (Gryaab rapport 2025:2).

Wunderlin, P., Bitterwolf, S. (2025). Micropollutant elimination in Swiss wastewater treatment plants: Experiences and developments. Swiss Water Association (VSA), Glattbrugg.

Xin, X., Kim, J., Weng, S. and Huang, C. H. (2024). Pilot Assessment of Impacts of Ozone and Ozone/Hydrogen Peroxide Treatment on the Fate of Per- and Polyfluoroalkyl Substances and Precursors. *ACS ES&T water*, 4(10), pp. 4545–4555. Available at: https://doi.org/10.1021/acsestwater.4c00565.

Appendix A

Table A1. Raw values from the column tests used to calculate the pressure drop per meter for GAC collected on 260318.

GAC depth (cm)	h_{ref} (cm)	h_{GAC} (cm)	L (cm)	Sample date
0	11.1	18.2	3.6	260318
0	11.1	18.2	3.6	260318
0	11.1	18.2	3.6	260318
25	11.1	15.8	3.6	260318
25	11.1	15.4	3.7	260318
25	11.1	15.4	3.7	260318
50	11.3	14.6	4.9	260318
50	11.3	14.5	5	260318
50	11.3	14.6	4.9	260318
75	11.3	13.5	6	260318
75	11.3	13.6	5.9	260318
75	11.3	13.7	5.9	260318
100	11.5	13.7	7.7	260318
100	11.5	13.8	7.6	260318
100	11.5	13.7	7.7	260318
150	11.1	13	7.6	260318
150	11.1	13.2	7.5	260318
150	11.1	13.3	7.4	260318
200	11.2	13.2	7.7	260318
200	11.2	13.2	7.7	260318
200	11.2	13	7.8	260318
250	11.2	13.2	7.9	260318
250	11.2	13.2	8	260318
250	11.2	13.1	7.9	260318
New	11.2	13.2	7.6	260318
New	11.2	13	7.7	260318
New	11.2	12.8	7.8	260318

Verification of Mini-column Tests

The mini-column tests were run once before the bed was lowered and then about a week and after more than one month after lowering of the bed. The GAC was collected at around 30% expansion for each experiment. However, the lower bed height meant the depths had to be read from the water surface level rather than the GAC surface level, so the max extraction depth was reduced to 230 cm, which is lower than the 250 cm used for the first test. Slight differences in bed expansion between the tests are expected, which can result in some differences in the exact collections depth especially for the deeper collection depths, but unlikely more than 10 cm, which is suggested by the similarity between results from 100 cm onwards for the last two tests.

During the mini-column tests, the flow rate was 72-74 ml/min, which is close to the desired flow rate, but it could cause small differences in the water head. Because the diameter of the centrifuge tubes tapers slightly along their length, the local velocity is dependent on the bed height. However, this effect was neglected. Regarding wall effects, the GAC has an average diameter of 1.1 mm and calculating the column to particle diameter ratio based on the top diameter of the tube yields around 25. To verify the method in relation to these assumptions and uncertainties, the same test was run with new GAC for each test. From Table A2. the results are in the same order of magnitude as from the manufacturer, which indicates the assumptions made for the mini-column test are reasonable and the testing procedure is successful in its purpose. Because the temperature of the incoming water was not kept exactly constant at 10°C, that could partially explain the differences between the tests for new GAC. For very small differences in hydraulic resistance, the mini-column test does not have sufficient resolution to discern differences.

Table A2. Pressure loss per meter bed from the manufacturer in comparison to those obtained during testing.

Sample date	Manufacturer value (mbar/m)	Calculated from experiments (mbar/m)
260318	~ 22 (at 7.5 m^3/h and 10°C)	23.0 ± 3.4
260330		22.9 ± 1.9
260504		20.2 ± 1.8

Table A3. Raw values from the column tests used to calculate the pressure drop per meter for GAC collected on 260330.

0	11.1	13.5	7.2	260330
0	11.1	13.4	7.3	260330
0	11.1	13.5	7.2	260330
25	11.2	13.1	7.5	260330
25	11.2	13	7.6	260330
25	11.2	13.2	7.5	260330
50	11.2	13	8	260330
50	11.2	13.2	7.9	260330
50	11.2	13.1	7.9	260330
75	11.2	12.9	7.9	260330
75	11.2	13	7.9	260330
75	11.2	12.9	7.9	260330
100	11.2	12.9	7.6	260330
100	11.2	12.7	7.7	260330
100	11.2	12.7	7.7	260330
150	11.2	13	8.6	260330
150	11.2	12.9	8.7	260330
150	11.2	12.8	8.7	260330
200	11.2	12.6	8.6	260330
200	11.2	12.5	8.5	260330
200	11.2	12.6	8.5	260330
230	11.2	12.6	8.7	260330
230	11.2	12.5	8.6	260330
230	11.2	12.5	8.6	260330
New	11.2	12.9	7.5	260330
New	11.2	13	7.6	260330
New	11.2	13	7.6	260330

Table A4. Raw values from the column tests used to calculate the pressure drop per meter for GAC collected on 260504.

0	11	17.8	5.9	260504
0	11	17.7	6	260504
0	11	17.7	6	260504
25	11.1	15.6	5.9	260504
25	11.1	15.2	6	260504
25	11.1	15.3	6	260504
50	11	14.9	7.2	260504
50	11	14.8	7.3	260504
50	11	14.9	7.2	260504
75	11	13.6	8	260504
75	11	13.7	8	260504
75	11	13.8	7.9	260504
100	11	12.7	8.2	260504
100	11	12.6	8.3	260504
100	11	12.6	8.3	260504
150	11.1	12.4	8.3	260504
150	11.1	12.3	8.3	260504
150	11.1	12.4	8.3	260504
200	11	12.3	8.4	260504
200	11	12.2	8.4	260504
200	11	12.2	8.4	260504
230	11	12.4	8.6	260504
230	11	12.2	8.7	260504
230	11	12.2	8.7	260504
New	11	12.6	7.7	260504
New	11	12.6	7.8	260504
New	11	12.6	7.8	260504

Appendix B

Table B1. Mass fractions for PSD based on mass GAC collected on 20260318.

Particle size interval (mm)	Mass 0 cm (g)	Mass 50 cm (g)	Mass 100 cm (g)	Mass 250 cm (g)
0-0.2	0	0	0	0
0.2-0.4	0.004	0.001	0	0
0.4-0.6	0.645	0.115	0.048	0.021
0.6-1.0	9.052	6.580	3.667	1.794
1.0-1.4	1.309	5.006	7.693	4.777
1.4-2.0	0.064	0.739	4.061	4.866
>2	0	0.009	0.201	0.527

Table B2. Mass fractions for PSD based on mass for new GAC.

Particle size interval (mm)	Mass (g)
0-0.2	0.007
0.2-0.4	0.067
0.4-0.6	1.333
0.6-1.0	7.830
1.0-1.4	7.963
1.4-2.0	3.703
>2	0.298

Validation of PSD Analysis – Moisture Absorption

To verify the assumption that moisture absorption by biomass was negligible for the PSD result, the 0 cm sample before lowering (20260318) was chosen as it was assumed to contain the most biomass because it exhibited the greatest hydraulic resistance in the mini-column tests. The total mass without drying the fractions was 11.074 g and with drying 10.831 g, a difference of 0.243 g. This suggests some water was accumulated, but the effect for the final distribution result was limited as can be seen in the Table B3. The difference is only between 0-0.04%, which suggests the assumption was reasonable, although not all samples were tested.

Table B3. The PSD results from GAC collected at the top (0 cm) from 20260318 with and without drying the fractions.

Particle Size Interval (mm)	Without drying (%)	With drying (%)
0-0.2	0	0
0.2-0.4	0.04	0.03
0.4-0.6	5.82	5.83
0.6-1.0	81.74	81.78
1.0-1.4	11.82	11.78
1.4-2.0	0.58	0.58
>2	0	0

Table B4. Mass fractions for PSD based on mass GAC collected on 20260330.

Particle size interval (mm)	Mass 0 cm (g)	Mass 50 cm (g)	Mass 100 cm (g)	Mass 250 cm (g)
0-0.2	0	0	0	0
0.2-0.4	0	0	0	0
0.4-0.6	0.007	0.004	0.005	0.002
0.6-1.0	4.888	2.426	1.791	1.407
1.0-1.4	7.942	8.402	6.359	6.648
1.4-2.0	1.692	3.886	4.949	7.018
>2	0.054	0.065	0.173	1.088

Table B5. Mass fractions for PSD based on mass GAC collected on 20260504.

Particle size interval (mm)	Mass 0 cm (g)	Mass 50 cm (g)	Mass 100 cm (g)	Mass 250 cm (g)
0-0.2	0	0	0	0
0.2-0.4	0	0	0	0
0.4-0.6	0.035	0.004	0.003	0
0.6-1.0	8.820	6.092	2.787	0.869
1.0-1.4	2.243	6.613	11.437	6.152
1.4-2.0	0.097	0.221	2.355	8.640
>2	0.003	0.008	0.024	1.052

Appendix C

Uncertainties in TSS Measurements and Validation

There were uncertainties during TSS analysis of the backwashing water. Although larger volume samples would have been preferred during filtration, the filters clogged at ca 5 mg residue. Therefore, only 3-4 mg could be filtered which makes instrument errors more significant, thus all samples for the mass balances were run in triplicates. Moreover, the influent and effluent TSS concentrations were twice verified at separate occasions. The influent TSS concentration was relatively close to what the influent turbidity sensor was reporting in the IBC, but not exact, see Table C3. However, because the influent TSS sensor was not fitted with a cleaning system until late, the values drifted to above the measuring range. Therefore, values from the turbidity sensor in the flow channel after the disc filters was instead used for calculations. The verification for the effluent turbidity sensor was less successful, see Table C4. TSS analysis is challenging at concentrations below 2 mg/L due to the limitations of analytical precision. Consequently, results in this low range carry significant uncertainty.

Table C1. The initial backwashing program used after the bed was lowered.

Backwash step	Duration (s)	Intensity (%)	Flow rate (m^3/h)
Air scoring	60	50	-
Mix (water only)	70	80	-
Water 1	240	-	16
Water 2	900	-	27
Total	1270		7.8

Table C2. Backwashing program with longer air scouring following used after 20260412.

Backwash step	Duration (s)	Intensity (%)	Flow rate (m^3/h)
Air scoring	180	60	-
Mix (air only)	180	60	-
Water 1	220-250	-	16
Water 2	1020	-	27
Total	1600-1630		8.6-8.7 m^3

Table C3. Comparison of influent TSS concentration from the turbidity sensor and from TSS analysis.

TSS turbidity sensor (mg/L)	TSS from analysis (mg/L)
6.1	4.8 ± 0.4
4.4	3.3 ± 0.5

Table C4. Comparison of effluent TSS concentration from the turbidity sensor and from TSS analysis.

TSS turbidity sensor (mg/L)	TSS from analysis (mg/L)
1.7	0.3 ± 0.1
1.1	0.1 ± 0.1

Table C5. TSS data for backwash on 2026-04-07.

Water phase	Filter (g)	Volume filtered (l)	Filter with residue (g)	Difference (g)	TSS (mg/L)
Water 1	0.1263	0.046	0.1295	0.0032	70
Water 1	0.1259	0.043	0.1282	0.0023	53
Water 1	0.1259	0.044	0.1293	0.0034	77
Water 2	0.1253	0.059	0.1272	0.0019	32
Water 2	0.1253	0.084	0.1278	0.0025	30
Water 2	0.1250	0.098	0.1284	0.0034	35

Table C6. TSS data for backwash on 2026-04-08.

Water phase	Filter (g)	Volume filtered (l)	Filter with residue (g)	Difference (g)	TSS (mg/L)
Water 1	0.1252	0.025	0.1307	0.0055	220
Water 1	0.1270	0.016	0.1303	0.0033	206
Water 1	0.1257	0.016	0.1285	0.0028	175
Water 2	0.1265	0.072	0.1304	0.0039	54
Water 2	0.1253	0.063	0.1288	0.0035	56
Water 2	0.1255	0.054	0.1286	0.0031	57

Table C7. TSS data for backwash on 2026-04-12.

Water phase	Filter (g)	Volume filtered (l)	Filter with residue (g)	Difference (g)	TSS (mg/L)
Water 2	0.1254	0.060	0.1304	0.0050	83
Water 2	0.1258	0.044	0.1293	0.0035	80
Water 2	0.1257	0.042	0.1290	0.0033	79
Water 2	0.1261	0.041	0.1292	0.0031	76
Water 2	0.1258	0.040	0.1288	0.0030	75

Table C8. TSS data for backwash on 2026-04-15.

Water phase	Filter (g)	Volume filtered (l)	Filter with residue (g)	Difference (g)	TSS (mg/L)
Water 2	0.1264	0.051	0.1291	0.0027	53
Water 2	0.1261	0.055	0.1294	0.0033	60
Water 2	0.1275	0.058	0.1307	0.0032	55

Table C9. TSS data for backwash on 2026-04-28.

Water phase	Filter (g)	Volume filtered (l)	Filter with residue (g)	Difference (g)	TSS (mg/L)
Water 2	0.1255	0.055	0.1284	0.0029	53
Water 2	0.1262	0.062	0.1288	0.0026	42
Water 2	0.1258	0.069	0.1291	0.0033	48

Table C10. TSS data for backwash on 2026-04-29.

Water phase	Filter (g)	Volume filtered (l)	Filter with residue (g)	Difference (g)	TSS (mg/L)
Water 2	0.1266	0.054	0.1297	0.0031	57
Water 2	0.1254	0.064	0.1285	0.0031	48
Water 2	0.1272	0.059	0.1299	0.0027	46

Table C11. TSS data for TSS profile for backwash on 2026-04-28.

Time into water phase (min)	Filter (g)	Volume filtered (l)	Filter with residue (g)	Difference (g)	TSS (mg/L)
0	0.1254	0.02	0.1298	0.0044	220
1	0.1263	0.02	0.1300	0.0037	185
2	0.1252	0.03	0.1292	0.0040	133
3	0.1244	0.061	0.1296	0.0052	85
4	0.1264	0.071	0.1291	0.0027	38
5	0.1252	0.1	0.1290	0.0038	38
6	0.1264	0.15	0.1299	0.0035	23
7	0.1257	0.15	0.1290	0.0033	22
8	0.1253	0.15	0.1286	0.0033	22
9	0.1255	0.2	0.1292	0.0037	19
10	0.1261	0.2	0.1291	0.0030	15
11	0.1259	0.2	0.1286	0.0027	13
12	0.1260	0.3	0.1293	0.0033	11
13	0.1262	0.3	0.1291	0.0029	10
14	0.1252	0.3	0.1279	0.0027	9
15	0.1269	0.3	0.1288	0.0019	6
16	0.1252	0.305	0.1274	0.0022	7